Journal of Infection 86 (2023) 421–438

Contents lists available at ScienceDirect

Journal of Infection

journal homepage: www.elsevier.com/locate/jinf

Systemic immune dysregulation in severe tuberculosis patients revealed by a single-cell transcriptome atlas

Yi Wang [a,*,1], Qing Sun [b,1], Yun Zhang [c,1], Xuelian Li [c], Qingtao Liang [c], Ru Guo [c], Liqun Zhang [c], Xiqin Han [c], Jing Wang [c], Lingling Shao [c], Yu Xue [d], Yang Yang [c], Hua Li [c], Lihui Nie [c], Wenhui Shi [c], Qiuyue Liu [e], Jing Zhang [d], Hongfei Duan [c], Hairong Huang [b], Laurence Don Wai Luu [f,1], Jun Tai [g,*], Xinting Yang [c,*], Guirong Wang [h,*]

[a] Experimental Research Center, Capital Institute of Pediatrics, Beijing 100020, PR China
[b] National Clinical Laboratory on Tuberculosis, Beijing Key Laboratory for Drug-Resistant Tuberculosis Research, Beijing Chest Hospital, Capital Medical University, Beijing Tuberculosis and Thoracic Tumor Institute, Beijing 101149, PR China
[c] Tuberculosis Department, Beijing Chest Hospital, Capital Medical University, Beijing 101149, PR China
[d] Department of Emergency, Beijing Chest Hospital, Capital Medical University, Beijing 101149, PR China
[e] Department of Intensive Care Unit, Beijing Chest Hospital, Capital Medical University, Beijing 101149, PR China
[f] School of Life Sciences, University of Technology Sydney, Sydney, Australia
[g] Department of Otorhinolaryngology Head and Neck Surgery, Children's Hospital Capital Institute of Pediatrics, Chinese Academy of Medical Sciences & Peking Union Medical College, Beijing 100020, PR China
[h] Department of Clinical Laboratory, Beijing Chest Hospital, Capital Medical University, Beijing Tuberculosis and Thoracic Tumor Institute, Beijing 101149, PR China

ARTICLE INFO

Accepted 28 March 2023
Available online 30 March 2023

Keywords:
Tuberculosis
Mycobacterium tuberculosis
ScRNA-seq
Severe patients
Immunological responses
Cytokine storm

SUMMARY

Tuberculosis (TB), caused by *Mycobacterium tuberculosis* (*Mtb*) infection, is currently the deadliest infectious disease in human that can evolve to severe forms. A comprehensive immune landscape for *Mtb* infection is critical for achieving TB cure, especially for severe TB patients. We performed single-cell RNA transcriptome and T-cell/B-cell receptor (TCR/BCR) sequencing of 213,358 cells from 27 samples, including 6 healthy donors and 21 active TB patients with varying severity (6 mild, 6 moderate and 9 severe cases). Two published profiles of latent TB infection were integrated for the analysis. We observed an obviously elevated proportion of inflammatory immune cells (e.g., monocytes), as well as a markedly decreased abundance of various lymphocytes (e.g., NK and γδT cells) in severe patients, revealing that lymphopenia might be a prominent feature of severe disease. Further analyses indicated that significant activation of cell apoptosis pathways, including perforin/granzyme-, TNF-, FAS- and XAF1-induced apoptosis, as well as cell migration pathways might confer this reduction. The immune landscape in severe patients was characterized by widespread immune exhaustion in Th1, $CD8^+$T and NK cells as well as high cytotoxic state in $CD8^+$T and NK cells. We also discovered that myeloid cells in severe TB patients may involve in the immune paralysis. Systemic upregulation of *S100A12* and *TNFSF13B*, mainly by monocytes in the peripheral blood, may contribute to the inflammatory cytokine storms in severe patients. Our data offered a rich resource for understanding of TB immunopathogenesis and designing effective therapeutic strategies for TB, especially for severe patients.

Introduction

Mycobacterium tuberculosis (*Mtb*), the causative agent of tuberculosis (TB), infects approximately one-quarter of the world's population.[1] It is the leading cause of death worldwide due to a single infectious agent with approximately 1.5 million deaths each year. Although the majority of *Mtb*-infected individuals are asymptomatic (latent TB infection, TBI), 5–10% of infected individuals will

Abbreviations: Tuberculosis, TB; *Mycobacterium tuberculosis*, Mtb; Latent TB infection, TBI; Intensive care unit, ICU; Peripheral blood mononuclear cells, PBMCs; B cell receptor, BCR; T cell receptor, TCR

* Corresponding authors.
E-mail addresses: wildwolf0101@163.com (Y. Wang), trenttj@163.com (J. Tai), yl-14t@163.com (X. Yang), wangguirong1230@ccmu.edu.cn (G. Wang).

[1] These authors contributed equally to this article.

https://doi.org/10.1016/j.jinf.2023.03.020

progress to active TB disease during their lifetime, with a range of lung and thoracic lymph node involvement or even extrapulmonary manifestations.[2]

In active TB (e.g., active pulmonary TB; PTB), many patients experience only mild or moderate symptoms, while some TB patients progress to severe disease or death. In particular, severe TB that requires ICU (intensive care unit) admission generally presents as respiratory failure, and despite the availability of effective therapies, mortality rates remain between 15.5% and 65.9%.[3] Therefore, it is important to understand the host immune response during TB disease to better design prognostic and diagnostic markers as well as to devise appropriate therapeutic interventions for TB patients with severe disease presentation.

Mtb infection and the anti-*Mtb* host immune response interact in vivo and shape disease severity as well as clinical outcomes, especially for severe TB cases. One of the major barriers in devising effective strategies to prevent and control *Mtb* infection is our incomplete understanding of the host-*Mtb* interaction. Thus, a comprehensive immune landscape, which characterizes the anti-*Mtb* and pathogenic immune responses in TB patients as well as dissect the potential changes related to disease severity, is urgently needed.

scRNA-seq (single-cell RNA sequencing), which is powerful at dissecting the immune responses, has been applied to study pathogen infections such as COVID-19.[4] Additionally, analysis of human peripheral blood immune cells can provide insights into the coordinated immune response to pathogen infections such as *Mtb*. Herein, we implemented scRNA-seq to obtain an unbiased visualization of the comprehensive immune responses in PBMCs (peripheral blood mononuclear cells) from patients with active TB with mild to severe symptoms, and patients in TBI stage as well as health controls (Fig. 1A). Our study depicts a high-resolution transcriptomic landscape of peripheral immune cells during disease progression of active TB, and we observed critical changes to severe TB patients, such as peripheral lymphopenia, significant activation of cell apoptosis pathways, widespread immune exhaustion, etc. Particularly, our data also presented a resource to unveil the features of cytokine storms in severe patients. Collectively, our findings will fill the gap in our comprehensive understanding of the pathogenic and protective immune responses of TB and provide potentially novel therapeutic targets, especially for severe TB patients.

Materials and methods

Study design and participants

Adults suspected to have TB were prospectively recruited and sampled at Beijing Chest Hospital (Beijing, China), which is the only national-level TB referral center in China. For TB cases, the inclusion criteria were: (1) with bacteriological evidence by culture or Xpert from sputum; (2) administered anti-TB drug for ≤3 days in the past 6 months. The exclusion criteria were: (1) had autoimmune disease; (2) had malignant tumors; (3) undergoing immunosuppressive therapy; (4) pregnant. For healthy controls, the inclusion criteria were: (1) negative for interferon gamma release assay; (2) with normal X-ray findings.

Clinical severity classification

X-ray or plain chest radiographs were obtained for all recruited patients. The radiographic extent of disease was graded into "Minimal," "Moderate" or "Advanced" stages, using a previously published decision tree,[5,6] based on the extent of lesions and presence of cavitation and pleural effusion. Minimal lesions: had only abnormal lymph node/hilar enlargement or cumulative area less than 1/3 of one lung, no cavitation, no effusion. Moderate lesions: had lesions of slight to moderate density of total extent not greater than 1/2 whole lung, or dense and confluent lesions occupying less than 1/3 of one lung, or cavitation up to 4 cm, or pleural effusion extending to less than within 2 cm of carina. Advanced lesions: lesion density exceeds criteria for moderate. The radiographic findings were combined with measures of inflammation (baseline levels of C reactive protein, CRP) and hypoxemia (peripheral pressure of oxygen, PO_2, or oxygen index) to define the disease clinical severity. Mild TB: had minimal lesions, or moderate lesions and CRP < 25 mg/L, $PO_2 \geq 80$ mmHg. Moderate TB: Moderate or Advanced lesions, and 25 mg/L ≤ CRP < 75 mg/L, and $PO_2 \geq 80$ mmHg. Severe TB: Advanced lesions, and CRP ≥ 75 mg/L, and PO_2 < 80 mmHg or oxygen index < 300 mmHg.

Sample collection

Supplementary Table 1 summarizes the characteristics of participants assessed in our study. The fresh blood samples from 6 healthy donors and 21 active TB patients (6 mild, 6 moderate and 9 severe patients) were immediately subjected to peripheral blood mononuclear cells (PBMCs) isolation using standard density gradient centrifugation. Cell viability was measured using the Countstar cell viability detection kit. The cell viability was > 90 % for each sample and thus underwent cell encapsulation to generate the 5′ gene expression profiles, B cell receptor (BCR) and T cell receptor (TCR) data using the 10 × Genomics single-cell transcriptome platform. Amplified cDNA was generated using a commercial emulsion-based microfluidic platform (Chromium 10×) and this cDNA was used for preparing both the single-cell RNA-seq libraries and BCR/TCR target enrichment and sequencing.

Single-cell RNA library preparation and sequencing

Using Chromium Single Cell 5′ Library, Gel Bead and Multiplex Kit, and Chip Kit (10× Genomics), cell suspensions were barcoded through the 10× Chromium Single Cell platform. Single-cell RNA libraries were prepared using the Chromium Single Cell 5′ Kit v2 (10× Genomics; PN-1000263), Chromium Single Cell V(D)J Reagent kits (10 × Genomics, PN-1000252(TCR), PN-1000253(BCR)) according to the manufacturer's instructions. The libraries were sequenced on the Illumina Novaseq 6000 sequencer (2 × 150 bp). Fastq files were generated using the CellRanger (v.5.0.0) mkfastq command.

Quantification and statistical analysis

Single-cell RNA-seq data analysis

Single-cell RNA-seq data were processed as previously described.[4,7] Briefly, raw and filtered gene expression matrices were generated using the kallisto/bustools (kb v0.24.4) pipeline. The filtered feature, barcode and matrix files were then analyzed in python (v3.8.10) using the anndata (ad) (v0.7.6) and scanpy (sc) (v1.7.2) packages. The data files of all 27 samples and previous scRNA-seq dataset of 2 PBMC samples from individuals with TBI were merged together using the ad.concat function.[8,9] Low-quality cells and potential doublets were then filtered and gene expression matrix were normalized by library size to 10,000 reads per cell as described in Wang et al.[9]

Gene features with high cell-to-cell variation in the data were prioritized using the sc.pp.highly_variable_genes function to select the consensus set of 1500 most highly-variable genes (HVGs) as previously described.[4] Integration of different datasets was performed as described in Wang et al.[9] using dimension reduction by principal component analysis (PCA) to 20 PCA components, batch effect correction by Harmony algorithm,[10] fast, sensitive and accurate integration of single-cell data with Harmony and unsupervised clustering using Louvain algorithm.[11,12]

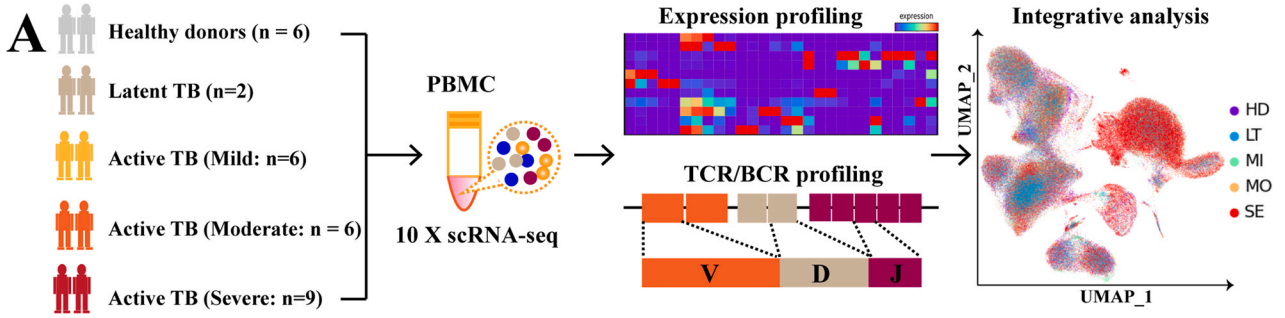

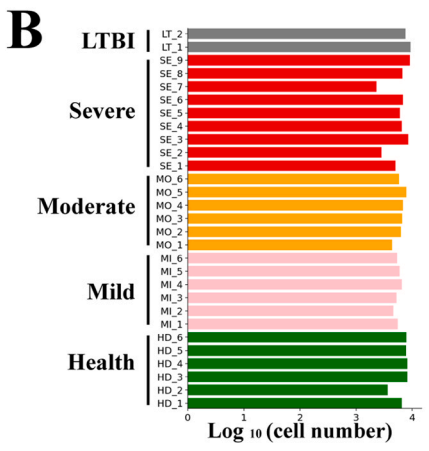

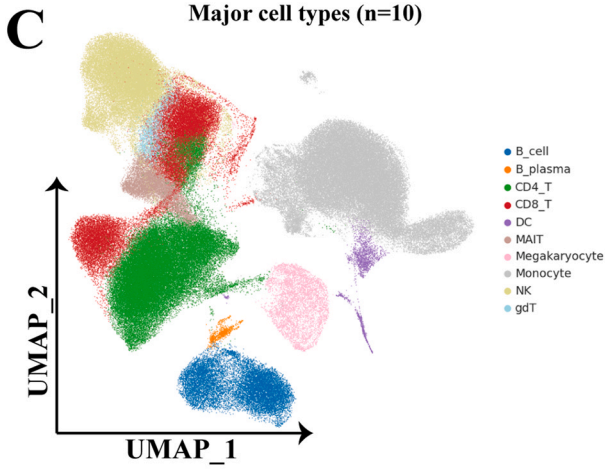

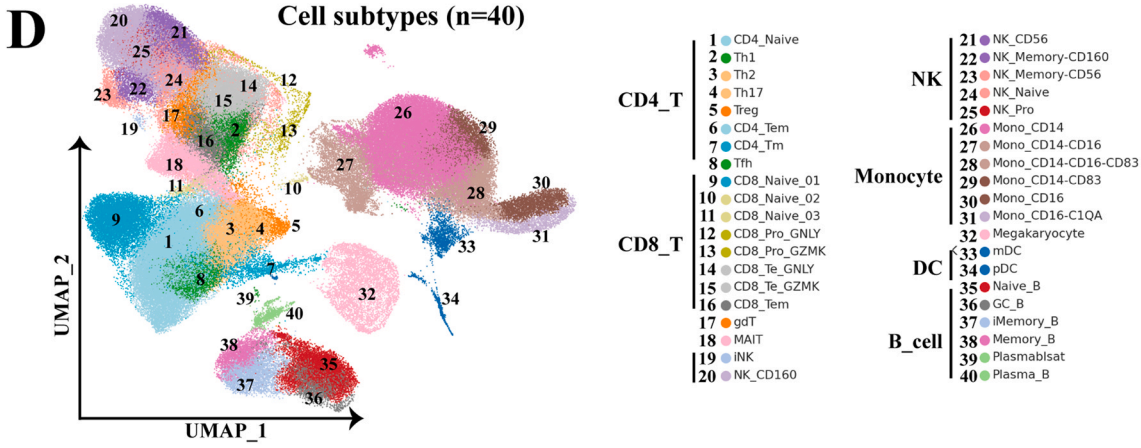

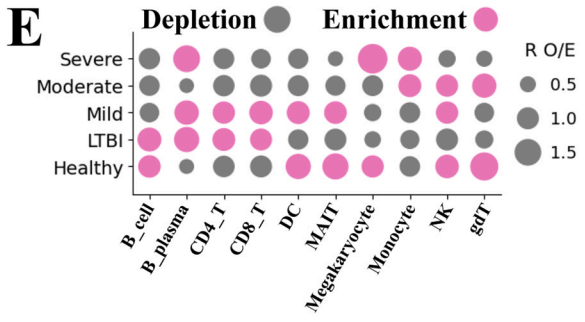

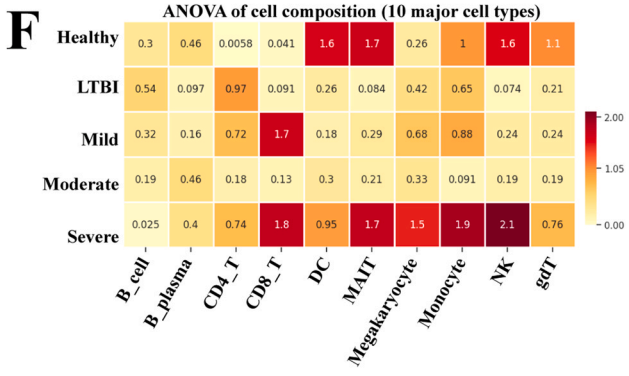

(caption on next page)

Fig. 1. Study design and overall results of single-cell transcriptional profiling of PBMCs from participants. A. Schematic diagram of the overall study design. 29 subjects, including 6 healthy donors, 21 active TB patients and 2 latent TB individuals. For the integrative analysis (right panel), the UMAP projection (Left) highlights the 5 conditional samples with different colors. Cells are colored according to the 5 conditions. B, Bar plot shows the $\log_{10}$ transformed cell number of each sample. Green represents six healthy donors, pink represents six active TB patients with mild disease, yellow represents six active TB patients with moderate disease, red represents nine active TB patients with severe disease, and gray represents two individuals with latent TB. C. The clustering result (Left row) of ten major cell types (right row) from 29 individuals. Each point represents one single cell, colored according to cell type. D. The clustering result (Left row) of 40 cell subtypes (Right row) from 29 individuals. Each point represents one single cell, colored according to cell type. E. Disease preference of major cell clusters estimated by $R_{O/E}$. F. Heatmap for q values of ANOVA for disease severity.

Cell clustering and annotations

Unsupervised clustering of cells was performed using sc.tl.louvain at different resolutions using the neighborhood relations of cells and consisted of two rounds. The first round (Louvain resolution = 2.0) identified 10 major cell types including $CD4^+$ T cells, $CD8^+$ T cells, gamma delta T cells, MAIT cells, NK cells, B cells, plasma B cells, monocyte cells, dendritic cells, Megakaryocytes. The second round (with Louvain resolution 2.0) subdivided $CD4^+$/$CD8^+$ T, B, monocyte, NK and DC cells into sub-clusters representing distinct immune cell lineages within each major cell type. Each sub-cluster was manually confirmed according to canonical marker genes. Cluster-specific signature genes were identified using the sc.tl.rank_genes_groups function. Cluster annotation was performed by manually matching canonical cell marker genes with Cluster-specific signature genes. Both canonical marker genes and cluster-specific highly expressed signatures are provided in the main text.

Cell state score of cell subtypes

Following cluster annotation, the overall activation level or physiological activity of cell clusters was compared using defined gene sets. The inflammatory response and exhaustion response gene sets were collected from published studies[4,13–15] while the Leukocyte Migration gene set (GO:0050900) was collected from the MsigDB database and previous reports.[13–15] The cytotoxicity score was defined using 17 cytotoxicity-associated genes (*PRF1*, *IFNG*, *GNLY*, *NKG7*, *GZMA*, *GZMB*, *GZMH*, *GZMK*, *GZMM*, *KLRK1*, *KLRB1*, *KLRD1*, *FCGR3A*, *FGFBP2*, *ZEB2*, *CTSW* and *CST7*). The cell state scores, defined as the average expression of the genes from the predefined gene set with respect to reference genes, were calculated using the Scanpy sc.tl.score_genes function. Comparison of the cell state score of one condition versus another condition was statistically tested using the t-test method.

TCR and BCR V(D)J immune repertoire sequencing and analysis

Following the manufacture's protocol (10× Genomic), full-length TCR/BCR V(D)J segments were obtained from amplified cDNA via PCR amplification from 5′ libraries using a Chromium Single-cell V(D)J Enrichment kit (10× Genomics, PN-1000005 (TCR), PN-1000016(BCR)). Demultiplexing, gene quantification and BCR/TCR clonotype assignment were conducted using Cell Ranger (v.6.0.0) *vdj* pipeline with GRCh38 as reference. V(D)J immune repertoire was analyzed by the python-toolkit Scirpy as previously described.[9]

Statistics

Statistical analysis and visualizations were performed in python and are provided with the results in the main text, in the figure legends or in the above Methods sections. The following symbols were used to indicate statistical significance for all figures:

ns: $p > 0.05$.
*: $p \le 0.05$.
**: $p \le 0.01$.
***: $p \le 0.001$.
****: $p \le 0.0001$.

Code availability

Experimental protocols and the data analysis pipeline used in this study follow the 10× Genomics and Scanpy official websites. Analysis steps, functions and parameters are described in detail in the Methods section. Custom scripts for analyzing data are available upon reasonable request.

Software and algorithms

Software	Source	Identifier
annadata	pypi	https://github.com/theislab/anndata
CellRanger v3.x	10 × Genomics	http://10xgenomics.com
ggplot	bioconductor	https://ggplot2.tidyverse.org
ggpubr	bioconductor	https://github.com/kassambara/ggpubr
gseapy-0.10.7	pypi	https://pypi.org/project/gseapy
harmonypy	pypi	https://github.com/slowkow/harmonypy
kallistobustools-0.24.4	pypi	https://github.com/pachterlab/kb_python Modular, efficient and constant-memory single-cell RNA-seq preprocessing. *Nat Biotechnol* **39,** 813–818 (2021).
scanpy v1.7.2	bioconda	https://github.com/theislab/scanpy
scirpy v0.7.0	bioconda	https://github.com/icbi-lab/scirpy
scrublet v0.2.3	pypi	https://github.com/swolock/scrublet
statannot	pypi	https://pypi.org/project/statannot

Results

Integrated analysis of TB scRNA-seq data

We generated single-cell transcriptome, TCR (T cell receptor) and BCR (B cell receptor) data from PBMCs (peripheral blood mononuclear cells) from 21 active tuberculosis (TB) patients with mild ($n = 6$), moderate ($n = 6$) and severe ($n = 9$) disease (Fig. 1). Controls included healthy donors (HDs, $n = 6$) and individuals with latent TB infection (TBI, $n = 2$). The single-cell transcriptional profiles for TBI were collected from a previous report.[8] Thus, the 29 participants were classified into five conditions: healthy donors (HD), TBI (LT), mild (MI), moderate (MO) and severe (SE). The laboratory findings and clinical features of 21 enrolled active TB patients are detailed in Table S1. We obtained in total 213,358 cells from 29 samples. Following computational doublet removal, 185,019 cells passed quality control (QC; see methods), including 125,444 cells from 21 active TB patients, 42,508 cells from 6 HDs and 17,067 cells from individuals with TBI. On average, there were 6400 cells from each PBMCs sample (Fig. 1B).

Following clustering, ten major cell types, including B cells, plasma B cells, $CD4^+$T cells, $CD8^+$T cells, NK (natural killer cells), DCs (dendritic cells), MAIT (mucosal-associated invariant T cells), monocytes, megakaryocytes and γδ T cells, were manually annotated based on the RNA expression of canonical marker genes and variable genes (Fig. 1C, Fig. S1, Table S2), with an additional 40 cell subtypes identified following subclustering (Fig. 1D, Fig. S1, Tables S3–7). Clusters unique to our data included two proliferating $CD8^+$ T cells, NK and monocyte cell subpopulations (Fig. 1D, Fig. S2, Tables S3–7). Cell clusters ($n = 10$) or subclusters ($n = 40$) reported here covered diverse cell types in the peripheral blood (Fig. 1B–C), and this information-rich resource was used for accurate annotation and analysis of these cell types at different resolutions (Fig. 1, Figs. S1–2, Tables S2–7).

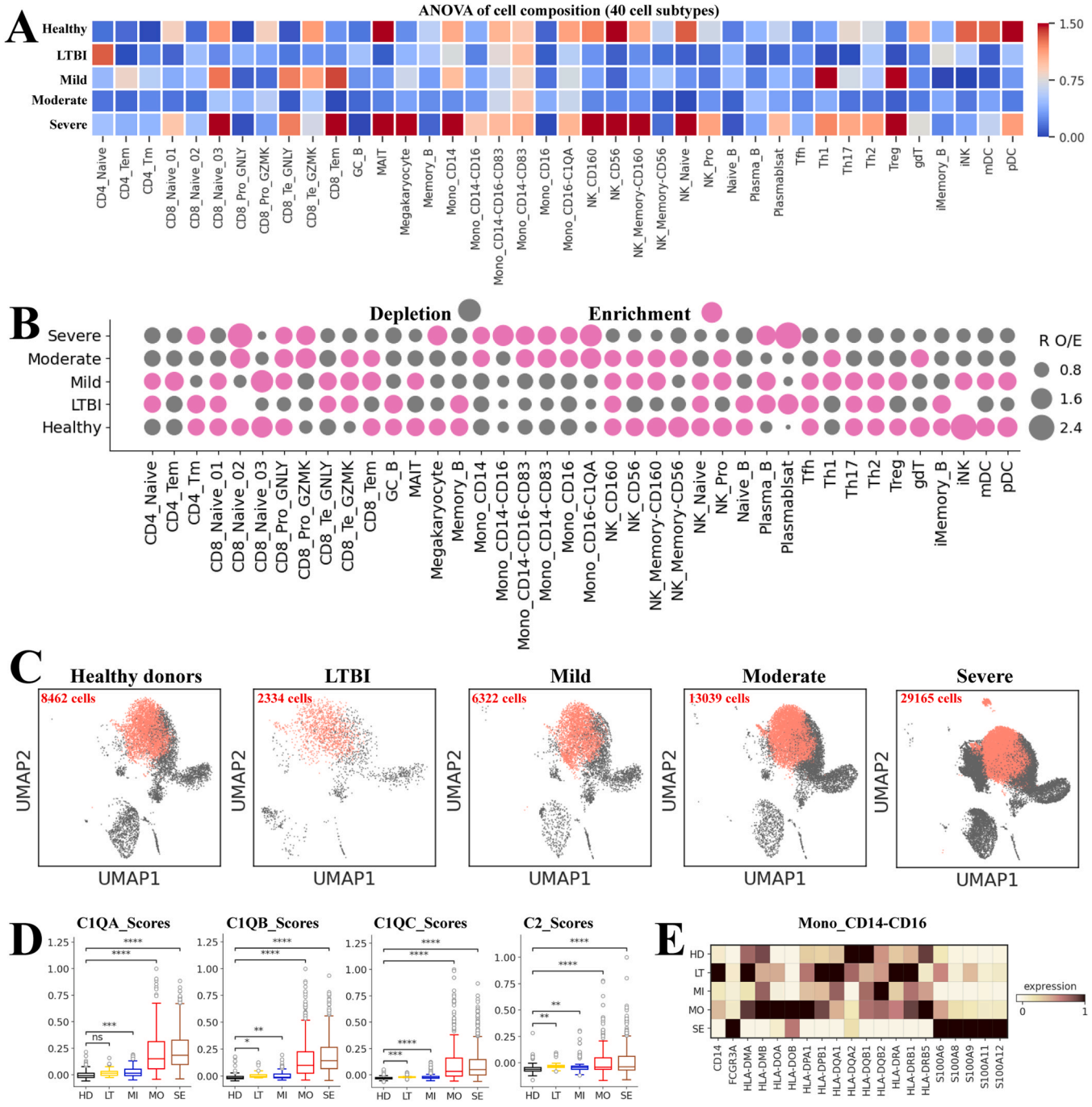

Fig. 2. Associations of TB severity with cellular compositions in PBMCs. A. Heatmap for q values of ANOVA. Disease severity: healthy donors, latent TB infection, mild, moderate and severe. B. Disease preference of 40 cell subclusters estimated by $R_{O/E}$. C. Density plots show the UMAP projection of peripheral Mono_CD14 cells from TB patients and healthy controls. D. Box plots of the expression of selected genes (C1QA, C1QB, C1QC, C2) in Mono_CD16-C1QA across conditions. E. Heatmap of normalized expression for selected genes in Mono_CD14–CD16 across conditions. Student's T-test was applied to test significance in D. *p < 0.05, **p < 0.01, ***p < 0.001, ****p < 0.0001, ^{ns}p > 0.05.

Obvious differences could be found based on uniform manifold approximation and projection (UMAP) (Fig. 1A). The disease preference of each major cell cluster was pictured based on $R_{O/E}$, i.e., the ratio of observed cell numbers to randomly expected cell numbers employed for eliminating the technical variations on disease preference estimation (Fig. 1E).[16] Notably, monocytes and megakaryocytes were more enriched in severe TB patients (Fig. 1E), and the frequency of monocytes in PBMCs could reach ~90% (SE_2) in severe TB patients, but none of the individuals in HD and LT conditions could reach 20% (Fig. S2). In contrast to monocytes and megakaryocytes that were increased in PBMCs, most immune cells, including DCs and various lymphocytes (e.g., NK, $CD4^+$T, $CD8^+$T, MAIT and γδ T cells), were seriously depleted in severe TB patients (Fig. 1E), suggesting lymphopenia in severe TB patients. Accordingly, increase of monocytes as well as decrease of various clusters of lymphocytes in severe TB patients has been supported by clinical blood cell counts (Table S1) and previous flow-cytometry-based analysis.[17,18] Likewise, we also employed analysis of variance (ANOVA) to dissect the associations of disease severity with the compositional changes of major immune cell clusters. Diverse innate immune cell clusters (e.g., NK, monocytes, megakaryocytes) were associated with TB severity, exhibiting obviously association with severe TB patients

(Fig. 1F). These results suggested that lymphopenia might be one prominent feature of severe TB patients.

Association of disease severity with various immune cell compositions

The information-rich resource enabled us to investigate the compositional changes in various cell subclusters, i.e., using $R_{O/E}$ analysis, and examine the associations of disease severity with the compositional changes of cell subtypes, i.e., using ANOVA analysis (Fig. 2, Fig. S3). After testing correction, significant associations were observed (Fig. 2A). Notably, most T and NK cell subsets were decreased in severe TB patients and showed obvious associations with severe disease (Fig. 2A–B). We first observed that Th1 and Th17 cell subtypes displayed obvious association with severe TB status (Fig. 2A). Th1 subtype highly expressed *TBX21* and *IFNG*, and Th17 highly expressed *CCR4*, *RORC* and *CCR6*, (Fig. S1, Table S3), validating both clusters as Th1 and Th17 cells, respectively. Both Th1 and Th17 cells were decreased in severe TB patients (Fig. 2B), which might lead to an inadequate Th1- and Th17-response in severe patients. Treg, marked by *FOXP3* and *IL2RA*, was also decreased and showed an association with severe patients (Fig. 2A–B), implying a potential imbalance immune response in severe TB individuals.

Diverse proliferative T and NK cell subtypes, characterized by high levels of *MKI67*, displayed different associations with TB severity (Fig. 2A). Two proliferative $CD8^+$T cell subsets were confirmed, with CD8_Pro_GNLY characterized by high GNLY and CD8_Pro_GZMK characterized by high GZMK and low GNLY, among others (Fig. S1). CD8_Pro_GNLY subset was enriched in active TB patients, particularly in those with severe disease (Fig. 2B, Fig. S3A), while CD8_Pro_GZMK was elevated in patients with moderate and severe disease (Fig. 2B, Fig. S4A). The increase of CD8_Pro_GNLY and CD8_Pro_GZMK clusters appeared to be derived from effector memory CD8 cells (CD8_Tem) and effector CD8 cells (CD8_Te_GZMK) based PAGA (partition-based graph abstraction) analysis (Fig. S4B).[7] CD8_Tem, expressing relatively high levels of *GPR183*, *S100A4*, *GZMA*, *GZMB*, *GZMH*, *GZMK* and *GNLY*, as a major source of proliferative $CD8^+$T cells, was decreased in severe TB patients and showed an obvious association with severe disease (Fig. 2A–B, Fig. S4A). This augment in proliferative $CD8^+$T cells and decrease in their precursor cells in severe TB patients partially suggested that those patients with severe disease might be relative to the dichotomous and incomplete adaptive immunity, particularly in $CD8^+$T cell-mediated immunity. One proliferative NK cell subset (NK_Pro) was identified and decreased in severe TB patients, which exhibited an association with those with severe disease (Fig. 2A–B, Fig. 4SC). The PAGA analysis indicated several nodes (e.g., NK_Pro cluster) with high connectivity between NK cell subtypes that suggested potential trans-differentiation bridges (Fig. S4D). Particularly, the proliferative NK cells appeared to be an intermediate state, which connected to all NK subsets with immature/naïve clusters to activated NK clusters (Fig. S4D). In addition, we also found high connectivity between NK_Pro and NK_CD160 as well as NK_Pro and NK_Naïve (Fig. S4D). These data inferred that NK_Pro may serve as intermediate cell populations in the PBMCs, which could be valuable for therapeutic means targeting NK_pro cells. In addition, NK_Naïve cluster, expressing high levels of *CCR7*, *SELL*, *LEF1* and *TCF7* genes, as a unique source of NK_Pro cells, were decreased and showed an association with severe TB patients (Fig. 2A–B, Fig. S4E). Taken together, the variations of proliferative cells, including proliferative $CD8^+$T and NK cell subsets, in distinct severity may suggest the complexity of $CD8^+$T and NK cell responses induced by *Mtb* infection, particularly in severe disease.

For myeloid cells, we found that their composition in severe TB patients differed from that of healthy controls, moderate, mild and TBI cases (Fig. 2A–B). In contrast to most T and NK cells that decreased in severe TB patients, most myeloid cell clusters enriched in TB patients with moderate and severe symptoms, particularly in those with severe disease (Fig. 2A–B). Mono_CD14 (classical $CD14^+$ monocyte), the largest monocyte cluster in PBMCs, was associated with severe TB patients and more enriched in this disease status (Fig. 2A–B). The differential UMAP projection patterns of Mono_CD14 cells between severe TB patients and other disease conditions (moderate, mild, TBI and healthy control) might suggest perturbed transcriptome features (Fig. 2C). Mono_CD16-C1QA cells, as the unique source of C1 complement components and the major source of peripheral complement components (Fig. S4F), showed an association with severe TB patients and significant enrichment in those with severe disease (Fig. 2A–B, Fig. S4G). Genes encoding complement components, especially for different C1Q chains (*C1QA*, *C1QB* and *C1QC*) and the C2 chain, were expressed at higher levels in *Mtb*-infected individuals (particularly in those with severe disease) compared to healthy donors (Fig. 2D), suggesting that the addition of *C1QA*, *C1QB*, *C1QC* and C2 to current biomarker panels might offer added value in the diagnosis of TB.[19] Importantly, patients with severe disease had the highest expression levels of genes encoding *C1QA*, *C1QB* and *C1QC* chains (Fig. 2D), indicating that *C1QA*, *C1QB* and *C1QC* might provide value in the prediction of disease severity.

Mono_CD14–CD16 cluster (intermediate $CD14^+CD16^+$ monocyte), which was elevated in severe TB patients, exhibited as an obvious association with severe disease (Fig. 2A–B, Fig. S4G). Particularly, decreased levels of HLA-DRA, HLA-DRB1 and HLA-DRB5 as well as increased levels of *S100A8*, *S100A9* and *S100A11* in Mono_CD14–CD16 from severe TB patients were observed (Fig. 2E), indicating that Mono_CD14–CD16 cells from severe TB patients were myeloid-derived suppressor cells (MDSCs). MDSCs are a population of heterogeneous immature myeloid cells which expand during inflammatory conditions to suppress T cell responses.[20,21] For peripheral blood, monocytic MDSCs (mMDSCs) exhibit the phenotype $CD14^+HLA\text{-}DR^{-/low}$, while CD14-expressing monocytes are HLA-DR positive.[22,23] Downregulation of HLA-II molecules, elevated calprotectin (e.g., *S100A8*, *S100A9*, *S100A11*), and immune-suppressive functions are hallmarks of MDSCs. Using the expression scores of HLA-II molecules (lower levels) and calprotectin (higher levels) vs the expression scores in healthy controls, TBI, mild and moderate patients, we identified that the Mono_CD14–CD16 subtype in severe TB patients highly resembled MDSCs (Fig. 2**E**). Other CD14-expressing monocytes including Mono_CD14, Mono_CD14–CD83 and Mono_CD14–CD16–CD83, did not display features of MDSCs in severe TB patients or *Mtb*-infected individuals (Fig. S4H). These results indicate that the emergence of MDSC-like monocytes (Mono_CD14–CD16) might be involved in the immune paralysis of severe TB patients.

Depletion of Th1 response and T cell exhaustion in severe TB patients

We then analyzed the expression features in T cells. Among the T cell subsets, Th1 cells are thought to play a key role in controlling *Mtb* infection by secreting cytokines such as IFN-γ and TNF. The expression of Th1 cytokine IFN-γ was significantly higher in mild, moderate and TBI conditions than in healthy controls, while the upregulated expression of IFN-γ was not observed in patients with severe disease (Fig. 3A). Similar results for IFN-γ expression were also observed in NK cells, which are another source of IFN-γ (Fig. 3B). Besides IFN-γ, TNF is involved in granuloma formation, and plays a crucial role in killing intracellular *Mtb* through reactive nitrogen intermediates together with IFN-γ.[24] In severe TB, the expression of TNF in Th1 and NK cells was not significantly upregulated compared to healthy controls, while its expression was significantly elevated in mild and moderate TB (Fig. 3A–B). Likewise, we also did not find increased expression of Th1 signatures in severe TB patients (Fig. 3C). These results indicate that lower levels of IFN-γ and TNF

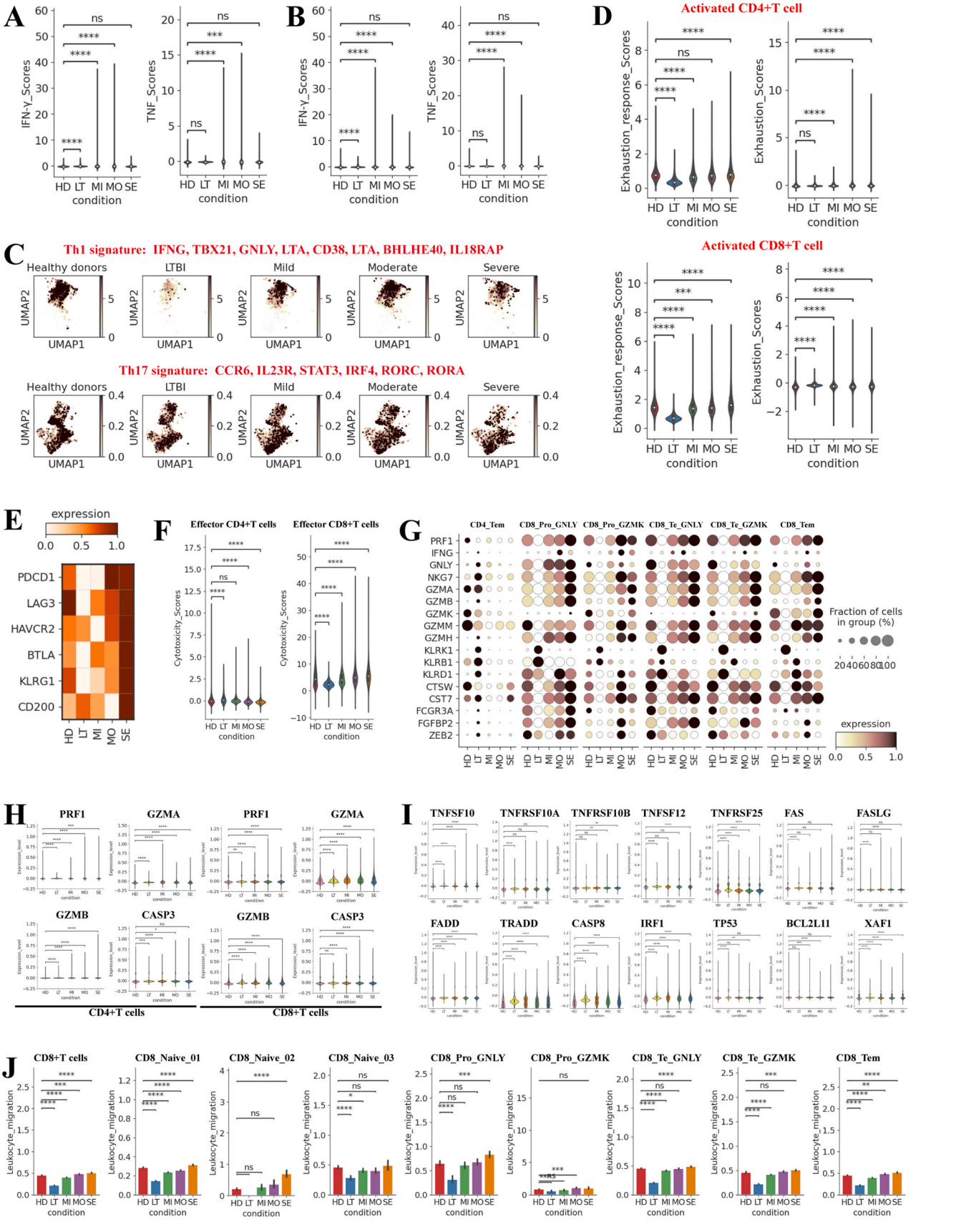

(caption on next page)

Fig. 3. Characterization of gene expression differences in CD4⁺ and CD8⁺T cells across five conditions. A. Violin plots of IFNγ (Left) and TNF (Right) gene expression in CD4⁺T cells across five conditions. B. Violin plots of IFNγ (Left) and TNF (Right) gene expression in NK cells across five conditions. C. Violin plots of exhaustion response scores and exhaustion scores in CD4⁺T (Left) and CD8⁺T (Right) cells across different conditions. D. UMAP plots of mean gene expression from Th1 (Top) and Th17 (Bottom) gene signatures, split by condition. E. Heatmap of normalized expression for selected exhaustion genes in Th1 cells across different conditions. F. Violin plots of cytotoxicity scores in effector CD4⁺T (Left) and effector CD8⁺T (Right) cell subtype per condition. G. Dot plots of the expression of selected genes in each CD8⁺T cell subtype per condition. H. Violin plots of the expression of perforin/granzyme-mediated apoptosis genes in CD4⁺T (Top) and effector CD8⁺T (Bottom) cells per condition. I. Violin plots of the expression of apoptosis genes in T cells per condition. J. Bar plots of the expression of leukocyte migration genes in CD8⁺T cells per condition. Student's T-test was applied to test significance in A, B, D, F, H and J. $^{*}p < 0.05$, $^{**}p < 0.01$, $^{***}p < 0.001$, $^{****}p < 0.0001$, $^{ns}p > 0.05$.

expression may contribute to the ineffective immune defense to *Mtb* infection in patients with severe disease.

Th17 cells secrete IL17, IL-17F, IL-21 and IL22 cytokines which stimulate defensin production and recruit monocytes and neutrophils to the site of inflammation. We did not observe elevated expression of Th17 cytokines and Th17 gene signatures in severe TB patients compared to these with mild and moderate disease (Fig. 3C, Fig. S5A), implying a potential dysfunction of Th17 response in severe disease. Th2 cells produce cytokines IL-4, IL-5, IL-13 and IL-25 which promote antibody generation but suppresses the Th1 immune response. We did not find significant differences in Th2-cytokine expression between active TB and healthy controls (Fig. S5B). Treg cells secrete IL-10 and TGF-β to downregulate CD4⁺T cell responses, inhibit T cell cytokine production, suppress the effector-immune response, and can induce *Mtb* dissemination and disease manifestation.[25] We also did not observe significant upregulation in active TB patients (Fig. S5C). These results suggest that depleted Th1 and Th17 immune response in severe patients may be not associated with Th2 and Treg immune suppression.

We next investigated the potential factors related with dysfunctional Th1 immune response in severe TB patients. Recent studies suggested that T-cells become dysfunctional in chronic pathogen infection, commonly referred to as immune exhaustion.[26,27] Here, we sought to explore the potential sources of T cell exhaustion in TB patients. We first defined an exhaustion response score and exhaustion score for each activated T cell based on the expression of the collected exhaustion response genes and reported exhaustion markers (Table S8), respectively, and used these two interrelated scores as indicators to evaluate the potential contribution to T cell exhaustion for each activated T cell subsets. We found significant upregulated expression of exhaustion response and typical exhaustion marker genes in activated CD4⁺T and CD8⁺T cells from active patients, especially in severe patients (Fig. 3D). Seven T cell subsets, including Th1, Treg, CD8_Pro_GNLY, CD8_Pro_GZMK, CD8_Te_GNLY, CD8_Te_GZMK and CD8_Tem, were detected with significantly higher exhaustion response and exhaustion scores based on our scRNA-seq data (Fig. S5D), suggesting these subsets might be major exhausted T cells.

Interestingly, Th1 cells, which play a cardinal role in protective immunity against *Mtb*, showed a higher exhaustion state in severe TB patients compared to all other conditions (Fig. S5D). Th1 cells in severe TB patients had high expression of multiple inhibitory molecules, including *PD-1*(*PDCD1*), *Tim-3* (*HAVCR3*), *BTLA*, *KLRG1* and *CD200* (Fig. 3E). In particular, *PD-1* interacts with *PDL-1*/*PDL-2*, Tim-3 with galectin-9 and *BTLA* with *HVEM* (also known as *TNFRSF14*), which recruits the tyrosine-protein phosphatase *SHP1* (also known as *PTPN6*) and/or *SHP2* (also known as *PTPN11*) by their intracellular domains (*ITIM*, immunoreceptor tyrosine-based inhibitory motif; *ITSM*, immunoreceptor tyrosine-based switch motif).[28] As such, the binding of inhibitory molecules in Th1 cells to their ligands could result in inhibition of LAT-Zap70 and PI3K-AKT signaling, leading to decreased cell proliferation and cytokine production (IFN-γ, TNF) (Fig. 3A). In addition, significant elevated expression of the key transcriptional factor *PRDM1* was found in *Mtb*-infected individuals compared with healthy donors (Fig. S5E). High *PRDM1* expression has been linked to increased inhibitory receptor expression and reduced polyfunctionality for exhausted cells.[27] Treg cells also showed a high exhaustion state in severe TB, while the roles of exhausted Treg cells will need further investigation. These data suggest that exhausted Th1 cells may play an important role in driving its immune dysfunction in severe TB patients.

Besides Th1 and Treg clusters, all activated CD8⁺ T cell subsets also had a high exhaustion state in active TB patients, particularly in severe disease (Fig. 3D, Fig. S5D). We found that activated CD8⁺ T cell subsets highly expressed those genes encoding surface inhibitory receptors (*PDCD1*, *LAG3*, *CTLA4*) in TB patients, especially in severe patients (Fig. 5SF). Furthermore, the expression of exhaustion-linked inhibitory molecules was not uniform across different activated CD8⁺T cell subsets with each exhausted CD8⁺T cells co-expressing multiple inhibitory receptors (Fig. S5G). CD8_Pro_GNLY highly expressed *TIGIT*, *LAG3* and *HAVCR2*, CD8_Pro_GZMK with *PD-1*, *TIGIT*, *LAG3*, *HAVCR2*, *BTLA* and *CD244*, CD8_Te_GNLY with *PD-1*, *CTLA4*, *HAVCR2*, *BTLA* and *CD80*, CD_Te_GZMK with *PD-1*, *LAG3*, *CTLA4* and *HAVCR2*, and CD8_Tem with *TIGIT*, *LAG3*, *CTLA4*, *HAVCR2*, *BTLA* and *CD80* (Fig. S5G). Similar to exhausted CD4⁺T cells, inhibitory receptors in exhausted CD8⁺T cells interact with their ligands (CD244 with CD48) to inhibit PI3K-AKT, LAT-ZAP70 and C3G-Rap signaling by recruiting *SHP1* and/or *SHP2*. This leads to decreased proliferative potential and cytokine production (e.g., IFN-γ).[29] Consistent with the results above, CD8⁺T cells in TB patients had a relatively lower expression of *IFNG* (Fig. S5H). In addition, elevated expression of *SPH1* and *PRDM1* was found in *Mtb*-infected individuals compared with healthy donors, particularly in severe patients (Fig. S5I). This may further enhance inhibitory receptor expression and reduce polyfunctionality in exhausted CD8⁺T cells. This data demonstrates that activated CD8⁺T cell subsets from active TB patients, especially for severe patients, had a high exhaustion status which might be associated with functional impairment in controlling *Mtb* infection.

We then evaluated the cytotoxicity scores of different effector T cell subsets across five conditions (Fig. 3 and Fig. S6). The effector CD4⁺T cell subset (CD4_Tem) showed higher cytotoxicity scores in TBI condition while patients in severe conditions had the lowest cytotoxicity scores (Fig. 3F). This implies that a higher cytotoxicity state in effector CD4⁺T cells might be related to more effective immune response to *Mtb* infection. In contrast, effector CD8⁺T cells showed higher cytotoxicity scores in active TB patients than healthy donors and TBI individuals at the bulk level, and patients with severe disease had the highest cytotoxicity status (Fig. 3F). Likewise, all effector CD8⁺ T cells showed an elevated trend of cytotoxicity scores in active TB patients, and two effector CD8⁺ T subsets, including CD8_Pro_GNLY and CD8_Tem, showed the higher cytotoxicity scores in severe TB patients (Fig. 3F, Fig. S6A). Effector CD8⁺T subsets from severe patients also overexpressed multiple cytotoxic genes, such as *PRF1*, *GNLY*, *NKG7*, *GZMA*, *GZMB*, etc. (Fig. 3G and Fig. S6B). Although effector CD8⁺T cells' cytolytic functions can directly kill *Mtb* or *Mtb*-infected cells via granule-mediated function (perforin, granzyme and granulysin),[30] these effector proteins can also lead to immunopathology by degrading the extracellular matrix and inducing inflammatory response.[31] Thus, overexpression of various cytolytic molecules in CD8⁺T cells may be associated with immunopathology in severe TB patients.

In addition to their role in the anti-*Mtb* response, cytolytic proteins (perforins and granzymes) also participate in pro-apoptotic response.[32] Here, expression of genes associated with perforin/granzyme-mediated apoptosis, including *PRF1*, *GZMA*, *GAMB* and *CASP3*, were analyzed.[33] Expression of *PRF1*, *GZMA*, *GAMB* and *CASP3*

was increased in CD4⁺T and CD8⁺T cells in active TB patients compared to healthy controls, and the higher expression of these genes was observed in severe TB patients (Fig. 3**H**). We also examined the expression of genes in other apoptosis-linked FAS, TNF and IRF1 pathways.[33,34] In T cell subsets, all TNF, FAS and XAF1 pathway members (*TNFSF10*, *FADD*, *XAF1*) showed an upregulated trend in active TB patients relative to healthy donors (Fig. 3I), although the expression of several apoptosis-related genes (*TNFRSF10A*, *FAS*) was not significant. In the TNF apoptosis pathway, activation of the TNF receptor by the TNF ligand results in binding to the adapter molecule TRADD with recruitment of another adapter protein called FADD. Similarly, activation of the FAS receptor with FAS ligand also results in FAAD binding.[33] FADD then binds to procaspase-8, resulting in activation of caspase-8 (CASP8) and apoptosis, which we observed to be significantly upregulated in T cell subsets for active TB patients (Fig. 3**I**). IRF1 triggers apoptosis under stress and forms a positive feedback loop with *XAF1* to upregulate target genes such as *CASP8*, *CASP1* and *TNF*.[34] *IRF1* and *XAF1* were both significantly upregulated in active TB patients (Fig. 3I). XAF1 can also enhance TP53-linked apoptosis via post-translational modification and *TP53* was increased in active TB patients, though not statistically significant for mild and severe patients. The key pro-apoptotic regulator BCL2L11 was also upregulated in active TB patients, particularly in severe TB patients (Fig. 3I).[35] These results suggest that upregulated genes relevant to the perforin/granzyme, TNF, FAS and XAF1 apoptosis pathways might lead to increased apoptosis of T cell subsets in TB patients, particularly in those with severe disease.

We also investigated the migration state of T cells using a migration scoring system (Fig. 3J, Fig. S6C–D). We found that CD4⁺T cells in active TB patients did not display a stronger migration status relative to healthy donors (Fig. S6C). In contrast, CD8⁺T cell subsets in severe patients likely underwent migration (Fig. 3J) and had highly expressed migration-associated genes like *CXCL10*, *CCL3*, *CXCL8*, *CXCL1,* etc. (Fig. S6D). The significant activation of migration pathways in peripheral CD8⁺T cells suggests that lymphocyte migration might be related to the reduction in CD8⁺T cell population in severe patients (Fig. 1**E**).

Clonal expansion in T cells and preferred usage of V(D)J genes in active TB patients

TCR information was detected in ~ 60% of T cells from the HD, MI, MO and SE conditions (Fig. 4A–B). The extent of clonal expansion in CD8⁺ T cells was larger (clonal size > 5) than in CD4⁺ T cells (Fig. 4D). After TB infection, T cell receptor β-chain constant domains 1 and 2 (TRBC1/2) percentage decreased, although not statistically significantly (Fig. 4C, S7A–B). TCR diversity as measured by alpha diversity showed no change after *Mtb* infection (Fig. 4E). The length distribution of the CDR3 region was similar for all conditions (Fig. 4F). The usage of IGH V(D)J genes across infection conditions was compared (Fig. S7C). A greater diversity of TCR V(D)J genes was observed in HD samples, while the overall diversity pattern decreased in MI, MO and SE samples. For example, in MI, the TRBJ1–3/TRBV28 V(D)J pair increased (60% of TRBJ1-3 recombination compared to < 15% in other conditions) while in SE, the TRBJ2-2/TRBV11-2V(D)J pair increased (30% of TRBJ2–2 recombination compared to < 10% in other conditions.

NK cells showed high cytotoxic and exhaustion state in TB patients

Except for the iNK cluster, all NK subsets from severe TB patients were enriched with multiple cytotoxic genes, such as *NKG7*, *GNLY*, *GZMA*, *GZMB*, *GZMH* and *CST7* (Fig. 5A, Fig. S8A), suggesting that the presence of an activated NK cell response is a feature of severe TB disease. The NK_CD56 cluster are robust producers of anti-*Mtb*-related cytokines such as IFN-γ and TNF.[36] Similar to our findings in Th1 cells, IFN-γ and TNF in the NK_CD56 cluster were significantly upregulated in mild and moderate patients relative to healthy donors, but not for severe patients (Fig. 5B). NK_CD160 cluster, which contribute to anti-*Mtb* host defense through cell-mediated cytotoxicity, displayed the highest cytotoxic state in severe TB patients compared to other conditions (Fig. 5C, Fig. S8B). Furthermore, NK_CD160 cluster from severe patients overexpressed multiple cytotoxic genes, such as *PRF1*, *NKG7*, *GZMA*, *GZMB*, *GZMH*, *CTSW* etc. (Fig. 5D). In addition to NK_CD160, other NK subsets, including NK_Pro, NK_Memory-CD56, NK_Memory-CD160 and NK_CD56, also displayed high cytotoxic state in severe patients (Fig. S8C). The high cytotoxic state of the NK subsets in severe patients may lead to immunopathology similar to CD8⁺T cells.

To further investigate differential transcriptomic changes in the NK cell subsets, we also evaluated the exhaustion, apoptosis and migration state of different NK cell subsets in active TB patients. Interestingly, except for immature NK cells (iNK), all other NK clusters in active TB patients were identified as exhausted NK cells with higher exhaustion response scores and exhaustion scores relative to healthy donors, particularly in severe patients (Fig. S8D). Compared to healthy donors, upregulated expression of multiple inhibitory molecules (e.g., *PD-1*, *LAG3*, *CTLA4*) was observed in exhausted NK cells in active TB patients, and patients in the severe condition overexpressed multiple inhibitory receptors (e.g., *PD-1*, *CTLA4*, *HAVCR2*, *BTLA*) and exhaustion-related molecules (e.g., *PTPN6*, *PTPN11* and *PRDM1*) (Fig. 5E). Similar to our observations in T cells, NK cell exhaustion may lead to reduction or loss of effector functions, and drive progression from mild or moderate disease to severe disease. In addition, we found that NK cells in severe patients likely underwent migration and apoptosis as evidenced by: (i) high migration scores (Fig. 5F); (ii) high expression of migration-related genes like *CXCL13*, *CXCL10*, *CCL3*, *CXCL1* and *CCL25* (Fig. 5F); (iii), high expression of genes in apoptosis-linked perforin/granzyme, FAS, TNF and IRF1 pathways (Fig. 5G). Significant activation of migration and cell apoptosis pathways in NK cells from severe patients indicates that NK cell migration and death might be related to the reduction in NK population, a phenomenon observed in patients with severe TB (Fig. 1E).

Relative to health controls, we found that genes encoding HLA class II molecules (HLA-DMA, HLA-DMB, HLA-DPA1, HLA-DPB1, HAL-DQA2, HLA-DQB1, HLA-DRA, HLA-DRB1, and HLA-DRB5) were significantly upregulated in *Mtb*-infected individuals (Fig. 5H–I). The extent of upregulation in HLA class II molecules tended to be greater in patients with severe TB. HLA class II upregulation is reflected in differentially regulated gene pathways, including increased crosstalk between NK cells and DCs. Likewise, we observed that genes encoding HLA-I class molecules were also significantly upregulated in severe patients relative other conditions (Fig. 5H), including non-classical HLA class I genes HLA-E, HLA-F and HLA-G, and canonical HLA class I genes HLA-A, HLA-B, and HAL-C (Fig. 5I).

Myeloid cells involved in the immune paralysis of severe TB patients

pDCs (plasmacytoid DCs) are characterized by classic markers such as *LILRA4*, *BLNK*, *ZFAT* and *IL3RA* (*CD123*) and expressed its major regulatory transcription factor *TCF4* (Fig. 6A).[37] CCR7, as an important chemokine receptor, is strongly upregulated upon exposure to TLR ligands and is critical for homing pDCs to lymph nodes.[38] We observed elevated expression of *CCR7* in TB patients, particularly in severe disease (Fig. 6A). pDCs specializes in microbial sensing and produces type I interferons in response to pathogens,[37] which thus expressed genes related to microbial sensing and induction of IFNs such as *IRF8*, *IRF7*, *IRF1*, *TLR7*, *PACSIN1* and *SLC15A4*. *IRF7* is the master regulator for IFN production in pDCs, while *IRF8* is essential for the development of pDCs and controls several functional modules in differentiated pDCs.[39] pDCs also expressed as

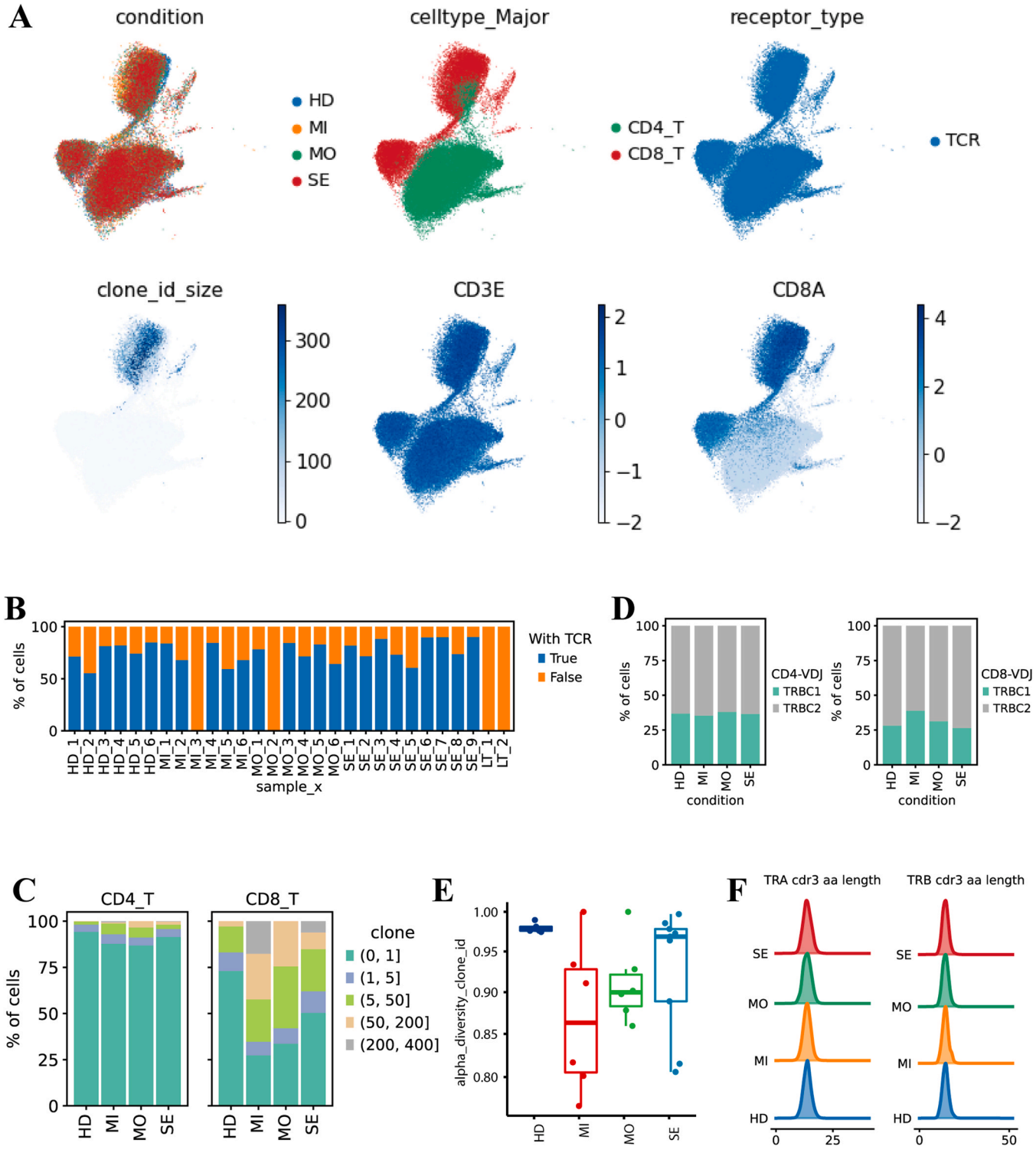

Fig. 4. Changes in TCR clones and selective usage of V(D)J genes. A. UMAP projection of T cells derived from PBMCs. Cells are colored by: conditions (Panel 1), B cell subtypes (Panel 2), if TCR detection was successful (Panel 3), clonotype expansion size (Panel 4), expression of T markers (Panels 5–6). B. Stacked bar plots showing the percentage of T cells with TCR information in each sample. C. Stacked bar plot showing the distribution of TRBC1 and TRBC2 in each T cell subtype. D. Stacked bar plots showing the clone state for each T cell subtype in each condition. E. Box plot of the alpha diversity value of clonotypes in each sample. Data points are grouped and colored by condition. F. Density curve plots showing the distribution shift of TRA and TRB chain CDR3 region length in TCR clone types for each condition.

genes associated with secretion of IFNs like *DERL3*. Our data suggested that, except for *IRF1*, the expression of these genes decreased as disease severity increased in active TB (Fig. 6A), implying that pDCs from severe TB patients may be dysfunctional in microbial sensing and IFN-I production. Relative to other conditions, pDCs in severe patients had lower expression of *SELL* (*CD62L*) and *NRP1* (Fig. 6A). *CD62L* is an adhesion molecule involved in trafficking pDCs to HEVs (high endothelial venules) while *NRP1* is involved in formation of primary immune synapse with T cells and positively regulates T cell proliferation.[40] In addition, *BCL11A*, an essential lineage-specific factor that regulates pDCs development, was decreased in active TB patients, particularly in severe patients,

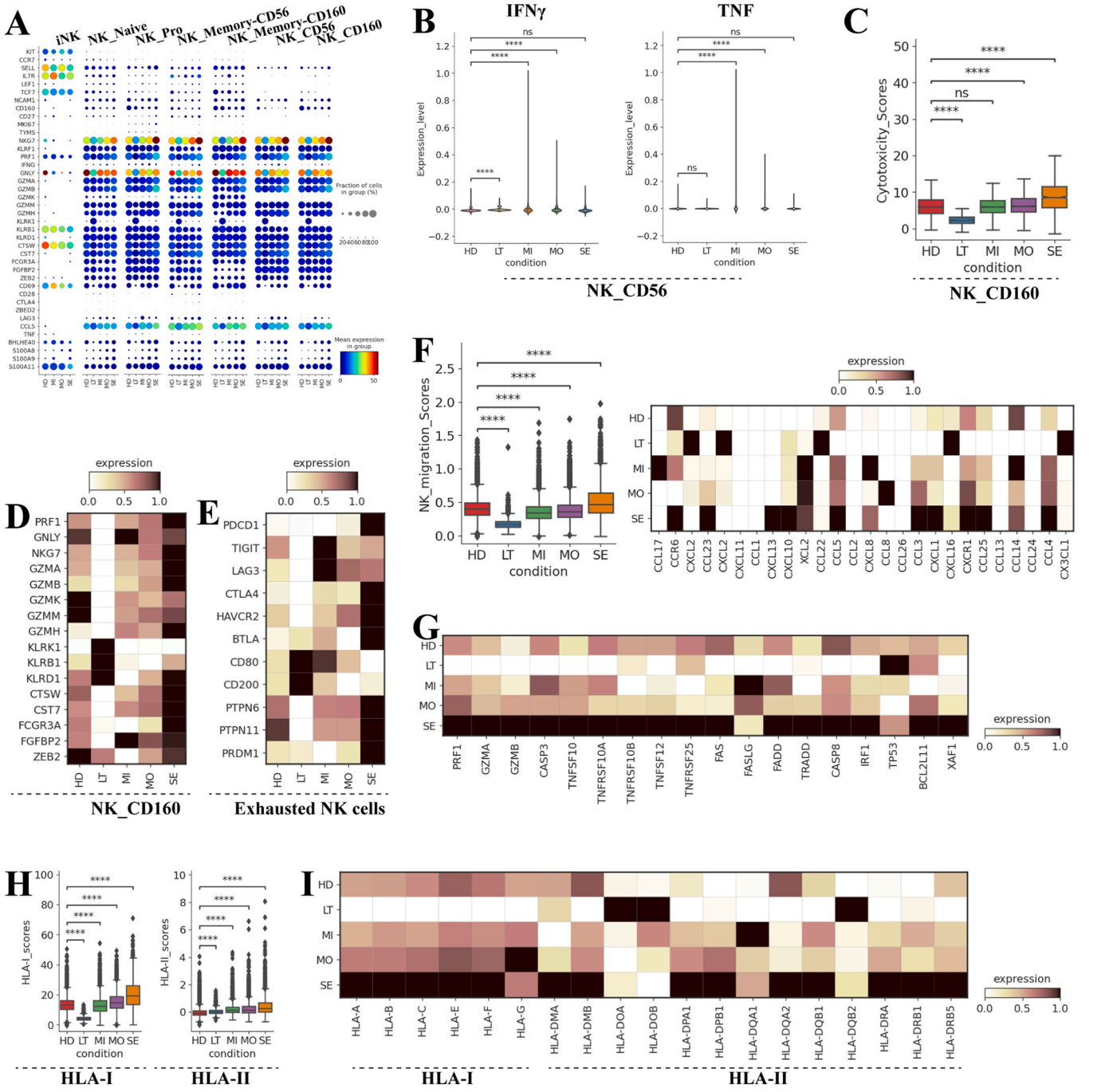

Fig. 5. Characterization of gene expression differences in NK cells across five conditions. A. Dot plots showing the expression of selected genes in each NK cell subtype per condition. B. Violin plots of IFNγ (Left) and TNF (Right) gene expression in NK_CD56 cells across conditions. C. Box plots of cytotoxicity scores in NK_CD160 cells across conditions. D. Heatmap of normalized expression for selected cytotoxicity genes in NK_CD56 cells across conditions. E. Heatmap of normalized expression for selected exhaustion genes in NK cells across conditions. F. Box plots of migration scores in NK cells across conditions (Left). Heatmap of normalized expression for selected migration-related genes in NK cells across conditions (Right). G. Heatmap of normalized expression for selected apoptosis-related genes in NK cells across conditions (Right). H. Box plots of HLA-I (Left) and HLA-II (Right) scores in NK cells across conditions. I. Heatmap of normalized expression for HLA-I and HLA-II genes in NK cells across conditions. Student's T-test was applied to test significance in B, C and F. *p < 0.05, **p < 0.01, ***p < 0.001, ****p < 0.0001, ^{ns}p > 0.05.

implying that pDCs in severe TB patients may have a hindrance in differentiation.[41] These results indicated that pDCs in severe patients may have a reduction in host response to *Mtb* infection.

mDCs (classical dendritic cells) expressed classic markers such as *CD1C*, *FCER1A*, *CLEC10A* and *ANXA1*, which were differentially expressed amongst the conditions (Fig. 6B). mDCs are specialized in antigen processing, and form a crucial interface between adaptive and innate immunity.[42] Many studies have shown that mDCs have a high expression of major histocompatibility complex (MHC) class II (HLA-DR) molecules, which are essential for antigen presentation. MHC-II molecules (e.g., HLA-DRA, HLA-DQA1) were significantly downregulated in the severe disease group relative to other conditions (Fig. 6B–C). Transcription factors (TFs) which control mDCs development such as *RELB*, *RBPJ* and *IRF4* were expressed at lower levels in active TB patients, especially in severe patients (Fig. 6B). Of note, IRF4 also controls other functional aspects in mDCs such as their migration and MHC presentation.[42] The loss of mDCs, down-regulation of MHC-II molecules and key TFs imply an immune

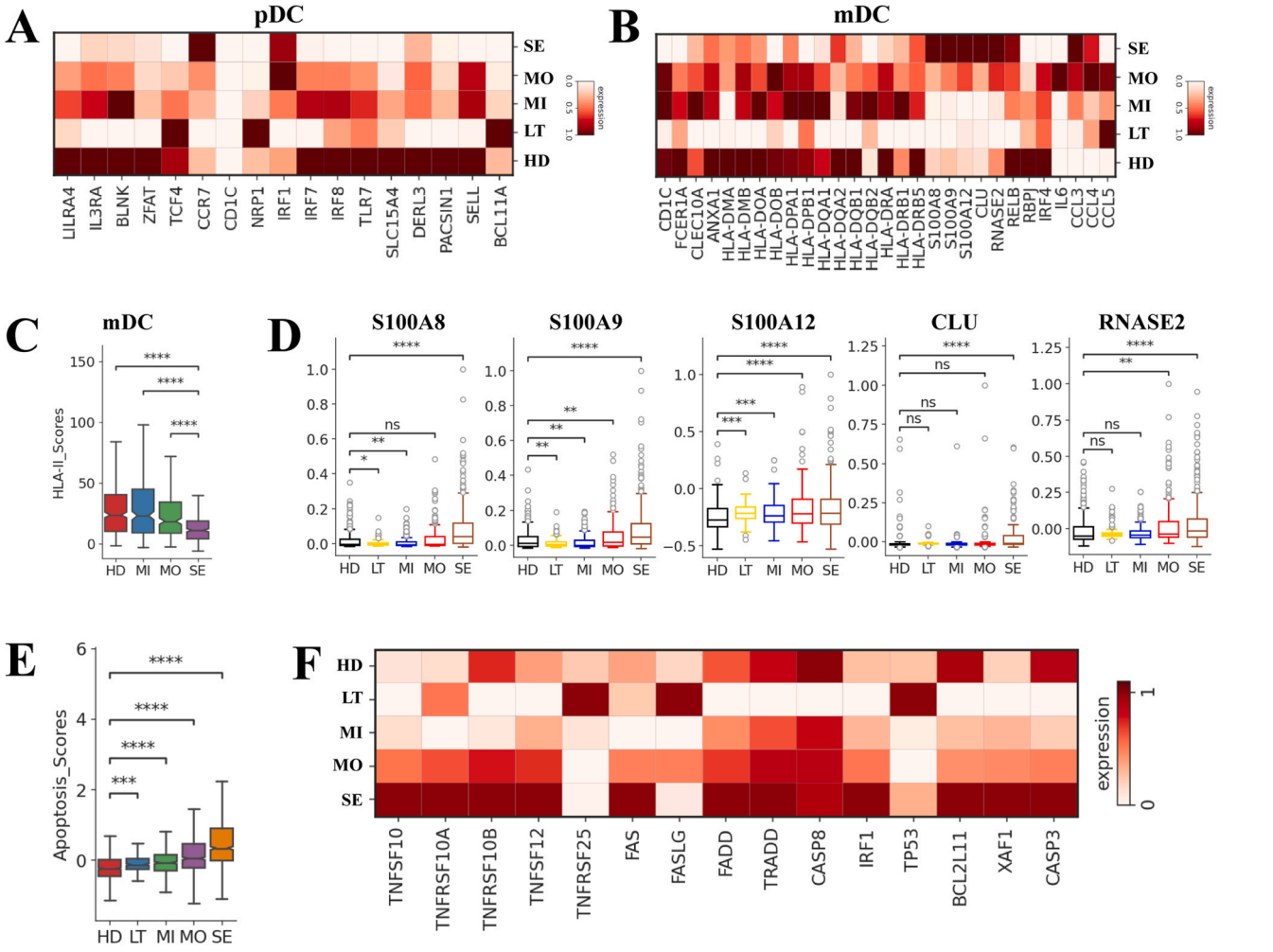

Fig. 6. Characterization of gene expression differences in myeloid cells across five conditions. A. Heatmap of normalized expression for selected genes in pDC across conditions. B. Heatmap of normalized expression for selected genes in mDC across conditions. C. Box plots of the expression of HLA-II genes in mDC across conditions. D. Box plots of the expression of S100A8/A9/A12, CLU and RNASE2 in mDC across conditions. E. Box plots of the expression of apoptosis genes in Mono_CD14–CD16 across conditions. F. Heatmap of normalized expression for apoptosis genes in Mono_CD14–CD16 across conditions. Student's T-test was applied to test significance in C, D and E. *p < 0.05, **p < 0.01, ***p < 0.001, ****p < 0.0001, ^{ns}p > 0.05.

paralyzed state of mDCs in severe TB patients (Fig. 2B, Fig. 6B). In addition, the genes related to neutrophil activation, such as *S100A12*, *S100A9*, *S100A8*, *CLU* and *RNASE2*, were expressed at higher levels in patients with severe disease compared to all other conditions (Fig. 6D). mDCs are prominent producers of proinflammatory chemokines and cytokines like *IL6*, *CCL3*, *CCL4* and *CCL5* after TLR ligand exposure.[43] The expression of these genes tended to upregulate in active TB patients (Fig. 6B). Overactivation of neutrophil and upregulation of proinflammatory molecules suggest that mDCs may be involved in the immunopathology of patients with severe TB.

Non-classical circulating monocytes (CD16^{+}) are more prone to undergo apoptosis in response to pathogen infection.[44] Consistently, we found that the apoptosis score for non-classical monocytes was significantly elevated in *Mtb*-infected individuals (TBI, mild, moderate and severe patients) relative to healthy donors, and those with severe TB had the highest apoptosis score (Fig. 6E), suggesting that non-classical monocytes in severe patients more likely underwent apoptosis. We observed that apoptosis-linked genes, such as *TNFSF10*, *TNFRSF10A*, *TNFSF12*, *FAS*, *FADD*, etc., were obviously upregulated in severe TB patients compared to other conditions (Fig. 6F), indicating that upregulated genes relevant to the TNF, FAS and XAF1 apoptosis pathways might lead to increased apoptosis of non-classical monocytes in those with severe disease. Taken together, these results suggest that non-classical monocytes in severe patients more likely undergo cell death.

Features of B cells in TB patients

Compared to T cells, the role of B cell-mediated immunity in protection against *Mtb* has been less studied. Naïve B cells from *Mtb*-infected individuals were enriched with activation genes like *IL4R*, *PAX5* and *BACH2* (Fig. S9A). Similar with Naïve_B subtype, two memory B cell subsets also did not express activation genes in *Mtb*-infected individuals such as *CD69*, *EBI3*, *TBX21*, *DHRS9* and *CD86* (Fig. S9A).[45] Relative to healthy donors, plasma B cells in active TB patients did not show higher expression of genes encoding the constant region of immunoglobulin G1 (IgG1), IgG2, IgG3, IgG4, IgA1 and IgA2 (Fig. S9A). These data indicate that key genes involving in B-cell-activation-related pathways, including somatic hypermutation, class switching, expansion and antibody production, were not enriched in active TB patients, implying that B and plasma cells in PBMCs might not be effectively activated.

Previous studies have demonstrated that cytokines produced by B cells can modulate T cell responses against intracellular pathogens; however, this has been less studied in *Mtb* infection.[46,47] Representative genes involved in T cell differentiation, expansion, and

anti-*Mtb* response (IL2, IL6, LTB, IL10, IFNG and IL10) were not enriched in B cells from TBI individuals and active TB patients (Fig. S9B).[48,49] In addition, B cells are also antigen-presenting cells which can capture and internalize antigens via surface immunoglobulins and then present them on their surface as MHC class II:peptide complexes to prime naïve CD4$^+$T cells.[50] Here, we investigated key genes associated with antigen presentation in B cells (Fig. S9A). Unexpectedly, compared to healthy donors, most B cell subsets had lower level of HLA-DRA, HLA-DRB1 and HLA-DRB5 in active TB patients. This data suggests that B cells in PBMCs may contribute to limited protection against *Mtb*. In addition, we found that expression of apoptosis-related genes (e.g., *TNFRSF10A*, *FAS*) was upregulated in active TB patients compared to healthy donors, particularly in severe patients (Fig. S9C).

BCR information was detected in > 80% of B and plasma cells from most samples (HD, MI, MO and SE). Clonal expansion (clonal size > 4) was observed in B_plasma cells from the MO and SE conditions (Fig. S10A, B, D). The largest portion of BCR in B cells was the IGHM subtype while the largest portion of BCR in plasma cells was IGHA1 and IGHA2 (Fig. S10C, S11A). The percentage of IGHM increased with disease severity in plasma cells but not in B cells (Fig. S10C). No differences were observed in the light chain type IGK and IGL in B and plasma cells (Fig. S11B). BCR diversity as measured by alpha diversity and the length distribution of the CDR3 region also showed no change (Fig. S10E, F). The usage of IGH V(D)J genes across infection conditions was compared (Fig. S11C). The combination of the most prevalent IGHJs and > 30 IGHV showed that TB infection induced many changes in IGH V(D)J genes (Fig. S11C). The V(D)J pair pattern was similar overall. The most prevalent pair in recombined IGHJ/IGHV, IGKJ/IGKV and IGLJ/IGLV regions was different.

S100A12 and TNFSF13B contributed to the cytokine storms in severe patients

We next explored the potential sources of cytokine production in TB. According to the expression of pro-inflammatory response genes and reported cytokine genes (Table S9),[51,52] we first defined an inflammatory and cytokine score for each cell subset and employed the two correlated scores as indicators to assess the potential contribution of each subset to inflammatory cytokine storm. We observed significant increased expression of inflammatory and cytokine genes in patients with severe disease (Fig. 7A, Fig. S12A), suggesting the presence of inflammatory cytokine storm in severe TB patients. Four major cell types, including monocytes, CD8$^+$T, NK and γδ T cells, had significantly elevated expression of inflammatory and cytokine genes in severe TB patients (Fig. S12B). At the granular level, sixteen subsets, including five monocyte subtypes (Mono_CD14, Mono_CD14-CD83, Mono_CD14–CD16–CD83, Mono_CD16, Mono_CD16-C1QA), five NK subtypes (NK_Pro, NK_Memory-CD56, NK_Memory-CD160, NK_CD56 and NK_CD160), five CD8$^+$T cell subsets (CD8_Naive_01, CD8_Naive_02, CD8_Pro_GZMK, CD8_Te_GZMK and CD8_Tem) and a γδ T cell subset, were identified with significantly higher inflammatory and cytokine scores and were thus defined as inflammatory cells. The higher scores suggest that these cells may be the dominant sources of inflammatory cytokine storm in severe TB patients (Fig. 7A, Fig. S12C–E). Among these defined inflammatory cells, CD14-expressing monocytes was the largest contributor and may be the major source for inflammatory cytokine storm (Fig. 7B). In contrast, megakaryocytes, which have been linked to inflammatory cytokine storms in other infectious diseases (e.g., COVID-19),[4] only displayed significantly higher cytokine score but not inflammatory score in severe TB patients (Fig. S12B).

We also investigated the proportion of these inflammatory cell subsets in TB patients. At the bulk level, we observed that the relative percentage of inflammatory cells tended to increase in TB patients with severe disease, though this was not significant (Fig. S13A). The proportion of most inflammatory cell subsets, including CD8_Naive_02, CD8_Pro_GNLY, CD8_Te_GZMK, NK_Pro, NK_Memory_CD56m, NK_CD160 and Mono_CD14–CD16–CD83, were enriched in severe TB patients (Fig. 2). The proportion of inflammatory cell subsets exhibited distinct enrichment patterns in severe patients, with CD14-expressing monocytes (Mono_CD14, Mono_CD14-CD83 and Mono_CD14–CD16–CD83) being highly enriched in all severe TB patients (Fig. S12B). Particularly, Mono_CD14, Mono_CD14-CD83 and Mono_CD14–CD16–CD83 may be the major peripheral sources driving the cytokine inflammatory storm in severe TB patients as evidenced by their high expression of inflammatory and cytokine genes and their increased cell proportion (Fig. 7A–B, Fig. S12, Fig. S13A–B). In addition to CD14-expressing monocytes, certain NK and CD8$^+$T cell subsets may also contribute to inflammatory cytokine storm in severe TB patients via enhanced expression of pro-inflammatory cytokines.

Next, we examined the inflammatory signatures for each inflammatory cell subset. Unique inflammatory cytokine gene expression was observed in each inflammatory cell subset (Fig. 7C, Fig. S13C), potentially indicating various mechanisms which induce inflammatory cytokine storms in severe TB. CD14-expressing monocytes had high expression of more cell-type-specific pro-cytokines (e.g., *S100A12*, *TNFSF13B*, *TNFSF13*, *FGF23*) (Fig. 7C), implying a central role for these three cell subtypes in triggering inflammatory cytokine storm. The Mono_CD14 subtype specifically expressed high levels of pro-inflammatory cytokines (e.g., *S100A12*, *TNFSF13B*, *FGF23*, *TNFSF10* and *SCYL3*) in severe patients (Fig. S13C). Mono_CD14-CD83 and Mono_CD14–CD16–CD83 also highly expressed specific pro-inflammatory cytokines in severe patients, such as *S100A12*, *TNFSF13B* and *FGF23*, etc. (Fig. S13C). In addition to CD14-expressing monocytes, other inflammatory cell subsets including NK and CD8$^+$T clusters, highly expressed *CCL5*, *SCYL2*, *IL32*, *CCL4* and *CCL4L2*, etc, in severe patients (Fig. 7C, Fig. S13C). The top 10 most highly expressed proinflammatory cytokines (*S100A12*, *TNFSF13B*, *FGF23*, *CCL5*, *SCYL3*, *TNFSF10*, *CCL4*, *IL32* and *TNFSF13*) contributed to ~99% of cytokine scores (Fig. 7D), indicating the core role of these cytokines in driving inflammation in severe disease. Among top 10 proinflammatory cytokines, *S100A12* and *TNFSF13B*, mainly secreted by inflammatory monocytes, may play central role in driving inflammatory cytokine storm in severe patients, because both cytokines contributed to ~76% of cytokine scores (Fig. 7D). Significantly upregulated expression of *S100A12* and *TNFSF13B* genes was observed in patients with severe disease (Fig. 7E), further validating findings in our scRNA-seq data analysis.

S100A12, as a member of pro-inflammatory Damage Associated Molecular Pattern molecules (DAMPs), was overexpressed during inflammation.[53] *S100A12* is a ligand of both RAGE (Receptor for advanced glycation end products) and TLR4 (Toll-like receptor), the former was validated to be a modulating factor, while the signal transduction is TLR4 dependent, facilitating proinflammatory activation.[53] Expression of TLR4 was significantly upregulated in severe TB patients relative to other conditions (Fig. 7E), especially for inflammatory monocytes (Fig. S13E), which was consistent with previous findings that proinflammatory *S100A12* was able to activate monocytes via TLR4.[53] TLR4 signaling primarily occurs through *MYD88* pathway, resulting in induction of pro-inflammatory cytokines.[54] Expression of *MYD88* also was significantly elevated in severe patients compared to other conditions, particularly in monocytes (Fig. 7E, Fig. S13E). These findings emphasize the importance of *S100A12* for design of potential therapeutic strategies to enhance protective immunity or decrease immunopathogenesis in severe TB patients. *TNFSF13B* was another important inflammatory cytokine in severe TB patients, and its levels were elevated in severe respiratory syncytial virus, bocavirus, influenza virus (H1N1) and *Mycoplasma pneumoniae* infections.[55] Likewise, we observed

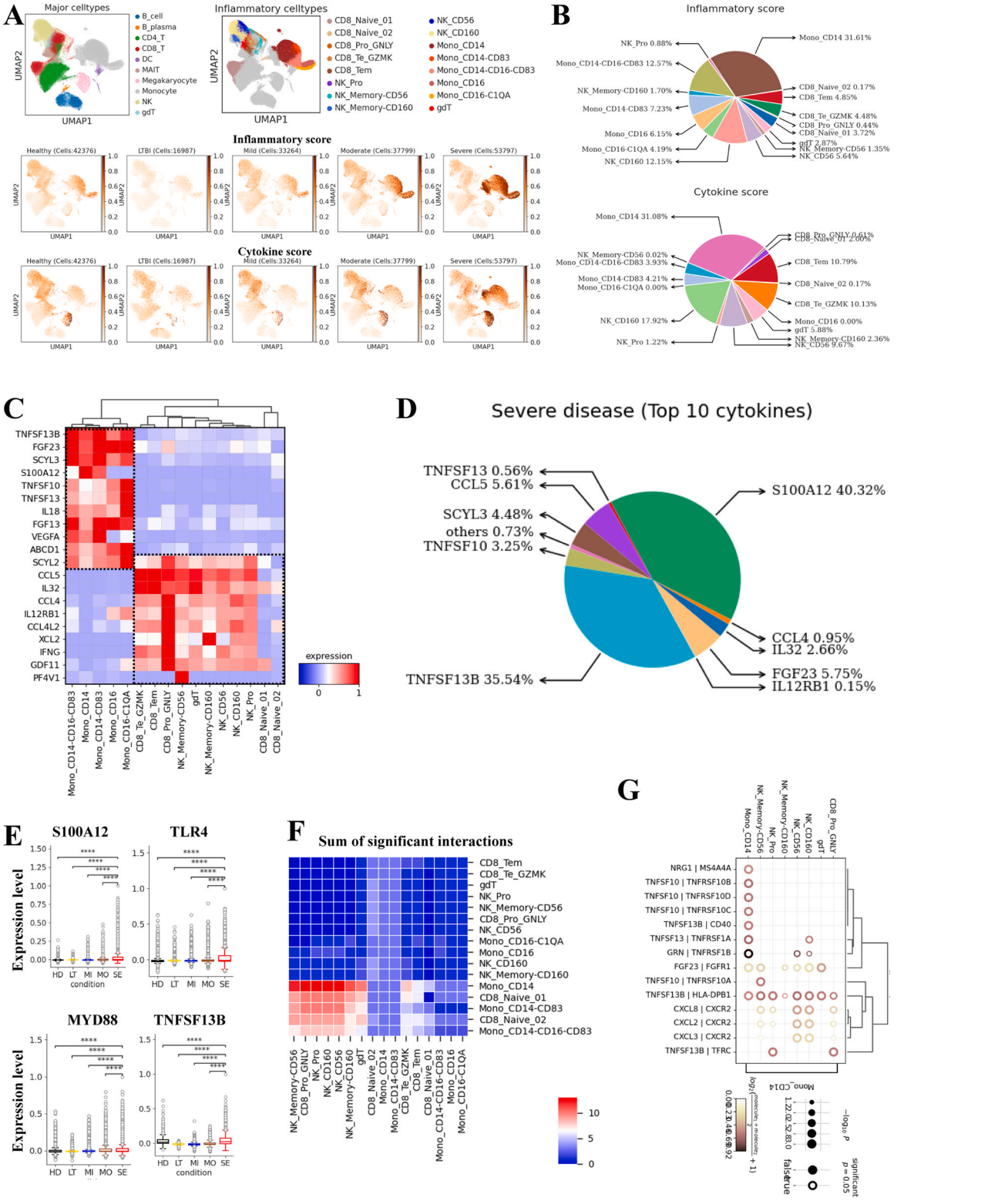

Fig. 7. *S100A12* and *TNFSF13B* contributed to the cytokine storms in severe patients. A. UMAP plots of PBMCs colored by: major cell types (Top left panel), inflammatory cell type (Top right panel), inflammatory score (Middle panel) and cytokine score (Bottom panel). B. Pie charts showing the relative percentage contribution of each cell type to the inflammatory score (Top panel) and cytokine score (Bottom panel). C. Heatmap of the cytokines expressed among 16 hyper-inflammatory cell subtypes. D. Pie charts showing the relative percentage contribution of top 10 cytokines in severe TB. E. Box plots showing the expression of selected genes in hyper-inflammatory cells across conditions. Student's T-test was applied to test significance. $^{*}p < 0.05$, $^{**}p < 0.01$, $^{***}p < 0.001$, $^{****}p < 0.0001$, $^{ns}p > 0.05$. F. Heatmap of the sum of signification interaction among 16 hyper-inflammatory cell subtypes. G. Dot plot of the interactions between Mono_CD14 and selected inflammatory cell types in severe TB patients. P values are indicated by the circle sizes, as shown in the scale on the right.

significantly increased expression of *TNFSF13B* in severe TB patients relative to other conditions (Fig. S13D). This cytokine could activate both noncanonical and canonical inflammatory signaling pathways, and formed a positive feedback loop to mediate an inflammatory environment and suppress anti-inflammatory mediators.[56] These observations suggested that the elevated *TNFSF13B* might be an important component involved in the formation of inflammatory storm in severe TB patients.

We reasoned that the systematic cytokine storm in severe patients may be related to cellular cross-talk via secreting diverse proinflammatory cytokines. To assess this, we investigated the ligand-receptor pairing patterns among hyper-inflammatory cell subtypes in severe samples within PBMCs (Fig. S13E). Our results revealed obvious ligand-receptor interactions of hyper-inflammatory cells in patients with severe disease (Fig. S13E). Interestingly, CD14-expressing monocytes in the peripheral blood of severe TB patients displayed much higher interactions with each other relative to inflammatory $CD8^+$T and NK cell subsets (Fig. 7F, Fig. S13E). CD14-expressing monocytes, particularly in Mono_CD14, expressed multiple receptors, implying that monocytes in severe patients could simultaneously receive multiple cytokine stimuli produced by other cell subsets (Fig. 7G, Fig. S13E–G). Interestingly, all inflammatory monocyte subsets expressed *CXCR2*, which receive *CXCL2*, *CXCL3*, *CXCL8* stimuli secreted by inflammatory cells (Fig. S13F). The interactions of inflammatory monocytes might mainly rely on TNFSF13B|TFRC, TNFSF13B|TFRC, FGF23|FGFR1, CXCL2|CXCR2, CXCL3|CXCR2 and CXCL8|CXCR2 (Fig. 7G**,** Fig. S13E–G). Taken together, these results validated the molecular basis for the potential cell-cell interactions in peripheral blood in severe TB patients.

Discussion

Tuberculosis (TB) poses a continuous threat to human health. Particularly, severe TB requires hospitalization or Intensive Care Unit (ICU) admission, and its mortality rates remain between 15.5% and 65.9%.[3] However, our current understanding of the host immune response to *Mtb* infection, especially for severe TB, is limited, making it difficult to design novel therapeutics. Here, we generated scRNA-seq data for 29 PBMC samples from 29 TB patients and healthy donors, constructed an information-rich data resource to dissect the immune responses of TB patients at the single-cell resolution and highlighted the immune characteristics of severe TB.

Ten major cell types and 40 cell subsets were clustered, offering fine details on the molecular and cellular response to *Mtb* infection. Overall, *Mtb* infection, particularly in severe TB patients, had a large impact on the composition of multiple immune cells. Our data highlighted impacts on lymphocyte populations, including NK, MAIT, γδT, $CD4^+$T and $CD8^+$T cells, and the dramatic reduction of number in lymphocytes was observed in TB patients with severe disease (Fig. 1 and Fig. S2). These data may support that lymphopenia is a key feature of severe TB patients. Although lymphopenia was found to affect various lymphocytes (e.g., NK, MAIT, γδT cells, etc.), our results indicated that severe TB had a preferential impact on NK cells (Fig. 1 and Fig. S2). NK cells and its subsets were significantly depleted in severe TB patients and showed an obvious association with severe disease (Fig. 1 and Fig. 2). In particular, we did not detect NK cells in 2 severe cases (SE_2 and SE_8), who had a worse clinical outcome (death), suggesting that there may be a correlation between NK cell depletion and clinical outcome (Fig. S2). It remains unclear why the lymphopenia in severe TB is NK cell biased, and the mechanisms of lymphopenia require further investigation. In contrast to lymphocytes that decreased in severe disease, a larger number of inflammatory-cell enrichments (e.g., monocytes and megakaryocytes) were observed in peripheral blood, implying that severe inflammation may exist in these patients. Notably, disease severity appeared to impact the diversity of TCR repertoires, which may have clinical implications.

T cells play a fundamental role in conferring protection against *Mtb* infection, while NK cells are increasingly regarded as an important component of the innate immune response to *Mtb,* linking adaptive and innate immunity.[57] However, persistent exposure or overexposure of antigens to T and NK cells can elicit a state of impairment in their function, referred to as immune exhaustion.[26] Our scRNA-seq data indicated that T (including $CD4^+$T and $CD8^+$T cells) and NK cells become dysfunctional in severe TB patients. Exhaustion of T and NK cells may be one explanation why patients with severe disease failed to control *Mtb* infection. Among the $CD4^+$T subsets, Th1 cells, which plays a key role in controlling *Mtb* infection, underwent exhaustion in severe TB patients and this was evidenced by (i) high exhaustion response and exhaustion scores; (ii) elevated expression of multiple inhibitory receptors (*PD1*, *Tim-3*, *BTLA*, *CD200*, *KLRG1*); (iii) decreased cytokine production (IFN-γ, TNF); (iv) augmented expression of exhaustion-related transcription factors (*Blimp-1*). As with Th1-cells, $CD8^+$T and NK cells also underwent exhaustion in severe TB patients, and displayed typical exhaustion features. It is noteworthy that exhausted Th1, $CD8^+$T and NK cells secreted lesser quantities of IFN-γ in severe TB patients. IFN-γ can activate macrophages and promote bacterial killing by permitting phagosomal maturation and production of reactive oxygen intermediates and antimicrobial reactive nitrogen intermediates.[58] Recent studies have shown that IFN-γ elicits autophagy in macrophages through the TLR, IRGM1 and PI3K signaling pathways, which increased the delivery of ubiquitin conjugates to the lysosome and enhanced the bactericidal capacity of the lysosomal soluble faction.[59,60] We found that T cells in severe TB patients had a weaker expression of Th1 gene signatures than mild and moderate individuals (Fig. 3), implying that macrophage from severe TB patients may not be adequately activated to clear or suppress *Mtb*. Importantly, we found that co-expression of multiple inhibitory receptors in exhausted Th1, $CD8^+$T and NK cells was a cardinal feature for severe TB patients. For instance, exhausted Th1 cells co-expressed PD1 together with *HAVCR2*, *BTLA*, *CD200* and *KLRG1* while exhausted NK cells co-expressed *PD1* together with *CTLA4*, *HAVCR2* and *BTLA*. It has been reported that the higher number of inhibitory molecules co-expressed by exhausted cells (T and NK cells), the more severe is the exhaustion.[28] Interestingly, these co-expression patterns are mechanistically relevant,[26,28] as simultaneous blockade by multiple inhibitory molecules in severe TB patients might result in synergistic reversal of T and NK cell exhaustion. There are several mechanisms by which inhibitory receptors and their ligands stimulate inhibitory signaling pathways: first, through the induction of inhibitory genes; second, by ectodomain competition, which involves inhibitory molecules sequestering target ligands and/or preventing the optimal formation of lipid rafts and microclusters; and third, through modulation of intracellular mediators, which can lead to local and transient intracellular attenuation of positive signals from activating receptors (e.g. TCR and its co-stimulatory receptors).[28] Hence, an in-depth understanding of the molecular mechanism by which T- and NK-cells undergo exhaustion during *Mtb* infection is critical in exploring novel therapeutic targets to protect the host from *Mtb*-induced damage.

According to our results, upregulated expression of multiple cytotoxic genes (e.g., *PRF1*, *GNLY*, *NKG7*, *GZMA*, *GZMB*) in effector $CD8^+$ T and NK cells may be involved in immunopathology in TB patients, particularly in severe TB, as these effector proteins (e.g., granzymes) could damage organs by degrading the extracellular matrix and inducing inflammatory response.[30,31,61] This result is not unexpected, because previous functional studies of exhausted cells (e.g., $CD8^+$T and NK cells) have suggested that unlike proliferative ability and cytokine production, cytotoxicity hallmarks were not diminished in exhausted cells.[62,63] In addition, upregulated perforin/granzyme

expression may also be related to increased T and NK cell apoptosis in TB patients by cooperating with other genes including *CASP3* and *CASP10*.[33] *CASP3* expression in TB patients was elevated in T and NK cells (Figs. 3 and 5), consistent with this hypothesis. Other apoptosis pathways including XAF1-induced apoptosis and extrinsic pathways of apoptosis (Fas/FasL) were also found to be activated in T and NK cells from severe TB patients. It was reported that XAF1 collaborates with *IRF1*, *CASP3*, *BCL2L11* and *TP53* to induce cell apoptosis. These genes were increased in T and NK cells from TB patients, including severe TB patients. Moreover, XAF1 can be induced by TNF and functions as an alternative path for TNF-related apoptosis.[33,34] In our study, we identified upregulated expression of genes involved in the extrinsic apoptosis pathways including *FAS*, *FASLG*, *FADD*, *TRADD* and *CASP8*. Taken together, our data suggest that upregulated genes associated with perforin/granzyme, *XAF1* and *FAS* pathways might result in T and NK cell apoptosis in TB patients, especially those with severe disease.

Myeloid-derived suppressor cells (MDSCs) are a population of heterogeneous immature myeloid cells which expand during inflammatory conditions and has the capacity of suppress T cell responses.[20,21] Interestingly, we identified a class of monocytic MDSCs (Mono_CD14–CD16) in the peripheral blood of severe TB patients which significantly increased. Consistent with the features of typical MDSCs, we observed increased calprotectin (*S100A6*, *S100A8*, *S100A9* and *S100A11*) and decreased HLA-II molecules in monocytic MDSCs. Due to MDSCs being associated with immune suppression, we speculate that monocytic MDSCs play a key role in inhibiting the immune response, amplifying TB pathogenesis and promoting severe disease progression. In addition to monocytic MDSCs, we observed a significant depletion of DCs, including pDCs and mDCs, which further indicates peripheral immune paralysis in severe TB patients. Together, our scRNA-seq data implies that myeloid cells may be involved in immune paralysis in severe TB patients.

In our attempt to investigate the potential cellular sources for inflammatory cytokines, we validated the presence of inflammatory cytokine storm in severe TB patients, which may be associated with increased disease severity and immunopathogenesis. Several monocytes, NK and $CD8^{+}$T subsets may be the main contributors of a diverse set of pro-inflammatory cytokines that were significantly increased in TB patients with severe disease progression. Further analysis indicated that *S100A12* and *TNFSF13B*, mainly secreted by monocytes, may play core role in driving cytokine storm in severe patients. Human *S100A12* was markedly overexpressed in inflammatory compartments (e.g., monocytes or granulocytes), and increased serum levels of *S100A12* were observed in patients suffering from various inflammatory, including infectious disease.[64] Consistently, our data validated that significantly elevated expression of *S100A12* was found in severe TB patients. Particularly, extracellular *S100A12*, as a pro-inflammatory protein, displays cytokine-like features, which is responsible for pro-inflammatory signaling through TLR4. Receptors (TLR4) for pro-inflammatory protein *S100A12* were also significantly upregulated in severe TB patients, particularly in inflammatory monocytes, which may increase *S100A12*-mediated inflammatory responses. Thus, blocking *S100A12* binding to its receptor TLR4 on TLR4 expressing cell lines, especially in monocytes, might abrogate the respective inflammatory signal, highlighting the value of S100A12-TLR4 pathway for development of potential therapeutic approaches in severe TB patients. As a result, TB patients with severe disease could benefit from treatment with anti-*S100A12* therapeutics, as attenuating *S100A12* production may blunt 'inflammatory cytokine storm.' In addition to *S100A12*, our scRNA-seq data showed that expression of *TNFSF13B* also was elevated in severe TB patients. We thus believe that upregulated expression of *TNFSF13B* may synergize with augmented *S100A12* to produce a strong inflammatory response, because this cytokine could activate both noncanonical and canonical inflammatory signaling pathways. This indicated that TB patients with severe disease may also benefit from *TNFSF13B* antagonist therapy.

Together, our scRNA-seq dataset, which includes samples from different disease severity, has uncovered multiple immune features of active TB that were not adequately appreciated previously. In particular, our data highlights the features of immune response and pathogenesis in severe TB patients, potentially assist the development of novel therapeutics.

CRediT authorship contribution statement

Yi Wang conceived the study; Yi Wang, Guirong Wang, Xinting Yang and Jun Tai designed the study; Yi Wang, Guirong Wang, Xinting Yang and Jun Tai supervised this project; Qing Sun, Yun Zhang, Xuelian Li, Qingtao Liang, Ru Guo, Liqun Zhang, Xiqin Han, Jing Wang, Lingling Shao, Yu Xue, Yang Yang, Hua Li, Lihui Nie, Wenhui Shi, Qiu Yue Liu, Jing Zhang and Hongfei Duan performed the experiments; Yi Wang, Hairong Huang, Xinting Yang, Guirong Wang and Jun Tai contributed the reagents, materials, and analysis tools.

Yi Wang performed the software; Yi Wang, Laurence Don Wai Luu, Qing Sun, Yun Zhang, Xinting Yang and Guirong Wang analyzed the data; Yi Wang drafted the original paper; Yi Wang, and Laurence Don Wai Luu revised and edited this paper; Yi Wang, Xinting Yang, Guirong Wang and Jun Tai reviewed the paper.

Transparency declaration

The lead author and guarantor affirm that the manuscript is an honest, accurate, and transparent account of the study being reported; that no important aspects of the study have been omitted; and that any discrepancies from the study as planned and registered have been explained.

Funding

This work was supported by grants from National Key Research and Development Program of China (Grant nos. 2021YFC2301101, 2021YFC2301102), Key Project of the Department of Science and Technology, Beijing, China (Grant nos. D181100000418003, Z191100006619078), Capital's Funds for Health Improvement and Research (2022-2-1132), Beijing Hospitals Authority's Ascent Plan (DFL20221102), National Natural Science Foundation of China (81970900), Public service development and reform pilot project of Beijing Medical Research Institute (BMR2021-3) and Beijing Public Health Experts Project (2022-3-040).

Availability of Data and Materials

Correspondence and requests for the data and materials should be addressed to Prof. Yi Wang (Capital Institute of Pediatrics) and Prof. Guirong Wang (Beijing Chest Hospital).

Competing interests

The authors declare no competing interests.

Acknowledgments

We thank all the participants. We thank for the Biological samples and data resource supported by Biobank of Beijing Chest Hospital. We gratefully acknowledge the participation of Beijing Digitf Biotechnology Co., Ltd. (Beijing) for the support of data analysis, Tongyuan Gene Co., Ltd. (Qingdao) for the support of cloud

computing platform, and NovelBio Co., Ltd. (Shanghai) for construction of single-cell sequencing Library, and thanks Dr. Yunke Li (Beijing Digitf Biotechnology) and Pengwei Hou (NovelBio) and Chao Wang (NovelBio) for their contribution.

Ethical Approval

The ethical approval for this study was obtained from the Beijing Chest Hospital ethics committee (Ethical approval no. YNLX-2022-006). Written informed consent was acquired from each participant.

Appendix A. Supporting information

Supplementary data associated with this article can be found in the online version at doi:10.1016/j.jinf.2023.03.020.

References

1. Organization WH. Global tuberculosis report 2021: supplementary material; 2022.
2. Horsburgh Jr CR. *Priorities for the treatment of latent tuberculosis infection in the United States. N Engl J Med* 2004;**350**:2060–7.
3. Duro RP, Figueiredo Dias P, Ferreira AA, Xerinda SM, Lima Alves C, Sarmento AC, et al. *Severe tuberculosis requiring intensive care: a descriptive analysis. Crit Care Res Pract* 2017;**2017**.
4. Ren X, Wen W, Fan X, Hou W, Su B, Cai P, et al. *COVID-19 immune features revealed by a large-scale single-cell transcriptome atlas. Cell* 2021;**184**:1895–913. https://doi.org/10.1016/j.cell.2021.01.053. [.e1819].
5. Berry MP, Graham CM, McNab FW, Xu Z, Bloch SA, Oni T, et al. *An interferon-inducible neutrophil-driven blood transcriptional signature in human tuberculosis. Nature* 2010;**466**:973–7. https://doi.org/10.1038/nature09247
6. Sousa J, Cá B, Maceiras AR, Simões-Costa L, Fonseca KL, Fernandes AI, Ramos A, et al. *Mycobacterium tuberculosis associated with severe tuberculosis evades cytosolic surveillance systems and modulates IL-1beta production. Nat Commun* 2020;**11**(1949). https://doi.org/10.1038/s41467-020-15832-6. [10.1038/s41467-020-15832-6[pii]].
7. Wang Y, Wang X, Jia X, Li J, Fu J, Huang X, et al. *Influenza vaccination features revealed by a single-cell transcriptome atlas. J Med Virol* 2022. https://doi.org/10.1002/jmv.28174
8. Cai Y, Dai Y, Wang Y, Yang Q, Guo J, Wei C, et al. *Single-cell transcriptomics of blood reveals a natural killer cell subset depletion in tuberculosis. EBioMedicine* 2020;**53**:102686.
9. Wang Y, Wang X, Luu LDW, Li J, Cui X, Yao H, et al. *Single-cell transcriptomic atlas reveals distinct immunological responses between COVID-19 vaccine and natural SARS-CoV-2 infection. J Med Virol* 2022;**1**. https://doi.org/10.1002/jmv.28012
10. Korsunsky I, Millard N, Fan J, Slowikowski K, Zhang F, Wei, et al. *Fast, sensitive and accurate integration of single-cell data with Harmony. Nat Methods* 2019;**16**:1289–96. https://doi.org/10.1038/s41592-019-0619-0
11. Traag VA, Waltman L, Van Eck NJ. *From Louvain to Leiden: guaranteeing well-connected communities. Sci Rep* 2019;**9**:1–12.
12. Levine JH, Simonds EF, Bendall SC, Davis KL, El-ad DA, Tadmor MD, et al. *Data-driven phenotypic dissection of AML reveals progenitor-like cells that correlate with prognosis. Cell* 2015;**162**:184–97.
13. Zhang JY, Wang XM, Xing X, Xu Z, Zhang C, Song JW, et al. *Single-cell landscape of immunological responses in patients with COVID-19. Nat Immunol* 2020;**21**:1107–18.
14. Wilk AJ, Rustagi A, Zhao NQ, Roque J, Martínez-Colón GJ, McKechnie JL, et al. *A single-cell atlas of the peripheral immune response in patients with severe COVID-19. Nat Med* 2020;**26**:1070–6. https://doi.org/10.1038/s41591-020-0944-y
15. Lee JS, Park S, Jeong HW, Ahn JY, Choi SJ, Lee H, et al. *Immunophenotyping of COVID-19 and influenza highlights the role of type I interferons in development of severe COVID-19. Sci Immunol* 2020;**5**:eabd1554.
16. Zhang L, Yu X, Zheng L, Zhang Y, Li Y, Fang Q, et al. *Lineage tracking reveals dynamic relationships of T cells in colorectal cancer. Nature* 2018;**564**:268–72.
17. Deveci F, Akbulut HH, Celik I, Muz MH, İlhan F. *Lymphocyte subpopulations in pulmonary tuberculosis patients. Mediat Inflamm* 2006;**2006**:089070. https://doi.org/10.1155/MI/2006/89070
18. Castaño D, García LF, Rojas M. *Increased frequency and cell death of CD16+ monocytes with Mycobacterium tuberculosis infection. Tuberculosis* 2011;**91**:348–60. https://doi.org/10.1016/j.tube.2011.04.002
19. Lubbers R, Sutherland JS, Goletti D, De Paus RA, Van Moorsel CH, Veltkamp M, et al. *Complement component C1q as serum biomarker to detect active tuberculosis. Front Immunol* 2018;**9**. https://doi.org/10.3389/fimmu.2018.02427
20. Gabrilovich DI, Nagaraj S. *Myeloid-derived suppressor cells as regulators of the immune system. Nat Rev Immunol* 2009;**9**:162–74. https://doi.org/10.1038/nri2506
21. Veglia F, Perego M, Gabrilovich D. *Myeloid-derived suppressor cells coming of age. Nat Immunol* 2018;**19**:108–19. https://doi.org/10.1038/s41590-017-0022-x
22. Bronte V, Brandau S, Chen SH, Colombo MP, Frey AB, Greten TF, et al. *Recommendations for myeloid-derived suppressor cell nomenclature and characterization standards. Nat Commun* 2016;**7**:12150. https://doi.org/10.1038/ncomms12150
23. Mengos AE, Gastineau DA, Gustafson MP. *The CD14(+)HLA-DR(lo/neg) monocyte: an immunosuppressive phenotype that restrains responses to cancer immunotherapy. Front Immunol* 2019;**10**:1147. https://doi.org/10.3389/fimmu.2019.01147
24. Cavalcanti YVN, Brelaz MCA, Neves JKDAL, Ferraz JC, Pereira VRA. *Role of TNF-alpha, IFN-gamma, and IL-10 in the development of pulmonary tuberculosis. Pulm Med* 2012;**2012**.
25. Dheda K, Schwander SK, Zhu B, Van Zyl-Smit RN, Zhang Y. *The immunology of tuberculosis: From bench to bedside. Respirology* 2010;**15**:433–50. https://doi.org/10.1111/j.1440-1843.2010.01739.x
26. Wherry EJ. *T cell exhaustion. Nat Immunol* 2011;**12**:492–9.
27. Crawford A, Angelosanto JM, Kao C, Doering TA, Odorizzi PM, Barnett BE, Crawford A, et al. *Molecular and transcriptional basis of CD4+ T cell dysfunction during chronic infection. Immunity* 2014;**40**:289–302.
28. Wherry EJ, Kurachi M. *Molecular and cellular insights into T cell exhaustion. Nat Rev Immunol* 2015;**15**:486–99.
29. Blackburn SD, Shin H, Haining WN, Zou T, Workman CJ, Polley A, et al. *Coregulation of CD8+ T cell exhaustion by multiple inhibitory receptors during chronic viral infection. Nat Immunol* 2009;**10**:29–37.
30. Lin PL, Flynn, JL. in Seminars in immunopathology. Springer, p. 239–49.
31. Hiebert PR, Granville DJ. *Granzyme B in injury, inflammation, and repair. Trends Mol Med* 2012;**18**:732–41.
32. Grotzke JE, Lewinsohn DM. *Role of CD8+ T lymphocytes in control of Mycobacterium tuberculosis infection. Microbes Infect* 2005;**7**:776–88.
33. Elmore S. *Apoptosis: a review of programmed cell death. Toxicol Pathol* 2007;**35**:495–516.
34. Jeong S-I, Kim JW, Ko KP, Ryu BK, Lee MG, Kim HJ, et al. *XAF1 forms a positive feedback loop with IRF-1 to drive apoptotic stress response and suppress tumorigenesis. Cell Death Dis* 2018;**9**:1–16.
35. Wang H, Han W, Guo R, Bai G, Chen J, Cui N. *CD8+ T cell survival in lethal fungal sepsis was ameliorated by T-cell-specific mTOR deletion. Int J Med Sci* 2021;**18**:3004.
36. Poli A, Michel T, Thérésine M, Andrès E, Hentges F, Zimmer J. *CD56bright natural killer (NK) cells: an important NK cell subset. Immunology* 2009;**126**:458–65.
37. Villani AC, Satija R, Reynolds G, Sarkizova S, Shekhar K, Fletcher J, et al. *Single-cell RNA-seq reveals new types of human blood dendritic cells, monocytes, and progenitors. Science* 2017;**356**:eaah4573.
38. Brandum EP, Jørgensen AS, Rosenkilde MM, Hjortø GM. *Dendritic cells and CCR7 expression: an important factor for autoimmune diseases, chronic inflammation, and cancer. Int J Mol Sci* 2021;**22**:8340. https://doi.org/10.3390/ijms22158340
39. Baccala R, Gonzalez-Quintial R, Blasius AL, Rimann I, Ozato K, Kono DH, et al. *Essential requirement for IRF8 and SLC15A4 implicates plasmacytoid dendritic cells in the pathogenesis of lupus. Proc Natl Acad Sci USA* 2013;**110**:2940–5.
40. Roy S, Bag AK, Singh RK, Talmadge JE, Batra SK, Datta K. *Multifaceted role of neuropilins in the immune system: potential targets for immunotherapy. Front Immunol* 2017;**8**:1228. https://doi.org/10.3389/fimmu.2017.01228
41. Ippolito GC, Dekker JD, Wang YH, Lee BK, Shaffer III AL, Lin J, et al. *Dendritic cell fate is determined by BCL11A. Proc Natl Acad Sci USA* 2014;**111**:E998–1006. https://doi.org/10.1073/pnas.1319228111
42. Mildner A, Jung S. *Development and function of dendritic cell subsets. Immunity* 2014;**40**:642–56. https://doi.org/10.1016/j.immuni.2014.04.016
43. Proietto AI, O'Keeffe M, Gartlan K, Wright MD, Shortman K, Wu L, et al. *Differential production of inflammatory chemokines by murine dendritic cell subsets. Immunobiology* 2004;**209**:163–72. https://doi.org/10.1016/j.imbio.2004.03.002
44. Castaño D, García L, Rojas López M. *Increased frequency and cell death of CD16+ monocytes with Mycobacterium tuberculosis infection. Tuberculosis* 2011;**91**:348–60. https://doi.org/10.1016/j.tube.2011.04.002
45. Horns F, Dekker CL, Quake SR. *Memory B cell activation, broad anti-influenza antibodies, and bystander activation revealed by single-cell transcriptomics. Cell Rep* 2020;**30**:905–13. [. e906].
46. Chan J, Mehta S, Bharrhan S, Chen Y, Achkar JM, Casadevall A, et al. *The role of B cells and humoral immunity in Mycobacterium tuberculosis infection. Semin Immunol* 2014:588–600. Elsevier.
47. Achkar JM, Chan J, Casadevall A. *B cells and antibodies in the defense against Mycobacterium tuberculosis infection. Immunol Rev* 2015;**264**:167–81.
48. Lund FE, Randall TD. *Effector and regulatory B cells: modulators of CD4+ T cell immunity. Nat Rev Immunol* 2010;**10**:236–47.
49. Mauri C, Bosma A. *Immune regulatory function of B cells. Annu Rev Immunol* 2012;**30**:221–41.
50. Kozakiewicz L, Phuah J, Flynn J, Chan J. *The role of B cells and humoral immunity in Mycobacterium tuberculosis infection. New Paradig Immun Tuberc* 2013:225–50.
51. Liberzon A, Birger C, Thorvaldsdóttir H, Ghandi M, Mesirov JP, Tamayo P, et al. *The molecular signatures database hallmark gene set collection. Cell Syst* 2015;**1**:417–25. https://doi.org/10.1016/j.cels.2015.12.004
52. Liu G, Jiang C, Lin X, Yang Y. *Point-of-care detection of cytokines in cytokine storm management and beyond: significance and challenges. VIEW* 2021;**2**(20210003). https://doi.org/10.1002/VIW.20210003
53. Foell D, Wittkowski H, Kessel C, Lüken A, Weinhage T, Varga G, et al. *Proinflammatory S100A12 can activate human monocytes via Toll-like receptor 4. Am J Respir Crit Care Med* 2013;**187**:1324–34. https://doi.org/10.1164/rccm.201209-1602OC
54. Bell E. *TLR4 signalling. Nat Rev Immunol* 2008;**8**. https://doi.org/10.1038/nri2301. [241-241].
55. Fan H, Lu B, Cao C, Li H, Yang D, Huang L, et al. *Plasma TNFSF13B and TNFSF14 function as inflammatory indicators of severe adenovirus pneumonia in pediatric patients. Front Immunol* 2021;**11**:614781.

56. Lawrence T. (Epub 2010/05/12. ⟨https://doi.org/10.1101/cshperspect⟩. a001651. PubMed PMID: 20457564).
57. Khader SA, et al. *Targeting innate immunity for tuberculosis vaccination. J Clin Investig* 2020;**129**:3482–91.
58. Kaufmann SH. *How can immunology contribute to the control of tuberculosis? Nat Rev Immunol* 2001;**1**:20–30.
59. Gutierrez MG, Master SS, Singh SB, Taylor GA, Colombo MI, Deretic V. *Autophagy is a defense mechanism inhibiting BCG and Mycobacterium tuberculosis survival in infected macrophages. Cell* 2004;**119**:753–66.
60. Alonso S, Pethe K, Russell DG, Purdy GE. *Lysosomal killing of Mycobacterium mediated by ubiquitin-derived peptides is enhanced by autophagy. Proc Natl Acad Sci USA* 2007;**104**:6031–6.
61. Wang Y, Huang X, Li F, Jia X, Jia N, Fu J, et al. *Serum-integrated omics reveal the host response landscape for severe pediatric community-acquired pneumonia. Crit Care* 2023;**27**:1–17.
62. Kusnadi A, Ramírez-Suástegui C, Fajardo V, Chee SJ, Meckiff BJ, Simon H, et al. *Severely ill patients with COVID-19 display impaired exhaustion features in SARS-CoV-2–reactive CD8+ T cells. Sci Immunol* 2021;**6**:eabe4782.
63. Sade-Feldman M, Yizhak K, Bjorgaard SL, Ray JP, de Boer CG, Jenkins RW, et al. *Defining T cell states associated with response to checkpoint immunotherapy in melanoma. Cell* 2018;**175**:998–1013. [. e1020].
64. Pietzsch J, Hoppmann S. *Human S100A12: a novel key player in inflammation. Amino Acids* 2009;**36**:381–9. https://doi.org/10.1007/s00726-008-0097-7